ONR-URI Composites Program
Technical Report No. 90-10

UIUC-NCCMR-90-10

NONLINEAR BEHAVIOR OF FIBER COMPOSITE MATERIALS AND ITS EFFECT ON THE POSTBUCKLING RESPONSE OF LAMINATED PLATES

Rami HajAli* and Su Su Wang**

December, 1990

National Center for Composite Materials Research
at University of Illinois, Urbana - Champaign
A DoD University Research Initiatives Center funded by the
Office of Naval Research, Arlington, VA

---

* Research Assistant

** Distinguished Professor, Dept. Mechanical Eng., University of Houston, Texas

ABSTRACT

The nonlinear stress-strain behavior of unidirectional fiber composite material was examined. Two approaches were adopted. The first approach considers the stress-strain as nonlinear elastic relations, which are derived at through the use of a complementary energy density function, and takes into account the material symmetry. The second approach adopts the Ramberg-Osgood representation of one-dimensional stress-strain curves. By utilizing the deformation theory to express the nonlinear parts of the strain, a nonlinear stress-strain behavior was obtained.

An incremental formulation of these theories was implemented in a finite element analysis. These approaches were examined in the context of postbuckling analysis of thick-section laminated plates. It is shown that the nonlinear behavior leads to a stiffness reduction for thick-section plates. Moreover, the models examined produce a close response for thick multi-layered laminated plates.

A-1

ACKNOWLEDGEMENT

This research was supported by the Lockheed Missiles & Space Company Inc. through the University of Illinois National Center for Composite Materials Research.

TABLE OF CONTENTS

1. INTRODUCTION

The design of fiber composite laminated structures has grown rapidly over the last two decades. These laminated anisotropic structures offer an exquisite alternative to the conventional isotropic materials due to their light weight to high strength ratio. Therefore, it is not surprising to find that the most immediate and primary applications of laminated structures were exclusive to the aeronautical and aviation industry in the form of thin laminated plates and shells. However, recently there has been a growing interest in the design and application of fiber-reinforced composite materials in the form of thick section plate and shell structures. This introduces a major concern when using methods of analysis, such as the classical laminate theory or its modifications, since these methods assume the presence of a plane stress field in each lamina. However, in a thick section composite, we verge to a true tridimensional stress state, especially if a need to analyze stress concentrations or structural discontinuities arises.

The search for effective and accurate design methods to analyze laminated structures has led to the use of complex models. These complexities arise through the consideration of geometric and material nonlinear behavior. Such models are assumed to produce a reliable and accurate design.

Recently, more attention has been directed towards exploring the effects of nonlinear constitutive behavior in the application of thermoset, thermoplastic and metal matrix fiber composite systems. These systems demand the application of a proper nonlinear constitutive theory. A nonlinear constitutive model can have a significant effect on the structural design, especially in the presence of local stress concentrations, such as crack tips, holes and cutouts, edge effects and structural discontinuities. Hence, it is important to assess such effects with the proper choice of constitutive relations.

This study is concerned with the formulation of a nonlinear constitutive model for fiber composite laminates. The nonlinear behavior of a single lamina, which results from the matrix nonlinear behavior or from a presence of micro-effects such as micro-cracks and imperfect fiber matrix interface, is introduced in the lamina's constitutive model.

In the first part of this report, two major theories and approaches of nonlinear constitutive models are examined and reviewed in a detailed manner. In the second part, an incremental formulation of the above theories is implemented. A nonlinear finite element analysis is performed to examine the above theories in the context of postbuckling analysis of thick section laminated plates. Discussion and recommendations follow.

2. LITERATURE REVIEW

2.1 Nonlinear Behavior of Fiber Composite Laminates

It has been well recognized that different fiber composite systems exhibit some form of nonlinear stress-strain behavior. One source of nonlinearity can be related to the matrix material, such as viscoelastic behavior in polymeric matrices or plasticity in metal matrices. Another source of nonlinearity can result due to micro-structural characteristics, such as micro-cracks or imperfect interface between the fiber and the matrix.

Several levels and approaches can be used in modeling the nonlinear behavior of fiber composites. A micromechanics approach can be obtained by modeling the micro-structure of the fibers and matrix inclusion in some form of periodical array subject to different states of stress and strain, Adams [1]. Another approach is to consider the nonlinear responses of a homogenized anisotropic lamina and to examine the nonlinear responses for the one dimensional average transverse stress and/or for the axial shear, while the stress-strain relation in the fiber direction remains linear. Finally, interaction terms of multiaxial stress states can be formed through the use of a potential stress function to describe the nonlinear parts of the strains, such as the stress energy density function or the deformation theory of plasticity.

Hashin et al [2] formulated and used this approach whereby they characterized the nonlinear stress-strain relations in a Ramberg-Osgood representation for the one dimensional average transverse and axial shear stress-strain relations. Moreover, they used the deformation theory of plasticity to form nonlinear constitutive relations which included an interaction term between nonlinear axial shear and transverse stresses.

Smith and Rivlin [3] considered a nonlinear polynomial form of the stress or strain energy density function, in which they reduced the polynomial basis by employing symmetry conditions on the basis form and by using some mathematical group theorems. It should be noted that this approach included major crystal classes of anisotropy.

The key idea in applying the above approach to anisotropic materials, is to extend the symmetry that a material exhibits in its crystallographic form to anisotropic bodies that are not crystals, but have a micro-structural symmetry, which results from the fiber periodic positioning in its inclusion, disregards the matrix or fiber materials.

Hahn and Tsai [4] followed this approach and considered the axial shear nonlinear behavior in a composite lamina under a plane stress state. They used a complementary elastic energy density function and imposed transverse-isotropy symmetry conditions to generate a nonlinear elastic constitutive relation. The interaction

terms between the shear nonlinear stress and other stress components were neglected in this formulation.

The theories of Hashin et al and Smith and Rivlin are reviewed and implemented in an incremental nonlinear finite element analysis in the following chapters.

2.2 Postbuckling Analysis of Laminated Plates

A flat plate subject to membrane forces remains flat provided these forces are small. By increasing the applied forces the flat plate becomes unstable and tends to deform in such configuration to allow small lateral displacements. These loads are the critical or buckling loads. If the loads are increased more, the plate establishes a stable configuration which allows bending due to membrane forces. The plate is then said to be in the postbuckling range and a stiffness reduction will occur, but the plate can still resist the increasing applied loads.

2.2.1 Nonlinear Analysis of Thin Laminated Plates

The involvement of geometric nonlinearity along with laminated plate theory makes it a tedious, if not impossible, task to generate close form solutions in the postbuckling range. The postbuckling formulations of thin flat plates involve the use of equilibrium equations written in the current deformed configuration, along with some Airy type function generating equilibrium

conditions in terms of the membrane forces. A second nonlinear equation is derived from the compatibility condition to form a set of two coupled nonlinear partial differential equations (PDE). This formulation of governing postbuckling equations for thin flat plates is introduced in Appendix B. These nonlinear PDE's can be solved approximately through the use of a truncated double Fourier series to generate a set of nonlinear algebric equations.

This approach was used by [5] to solve a postbuckling of orthotropic rectangular plate with all-clamped or all-simply supported edges. Also [6] considered a postbuckling of symmetrically laminated plates with the same boundary conditions as [5].

2.2.2 Nonlinear Analysis of Thick Composite Laminate

The analysis of thick section laminated plates and shells includes the account for transverse shear which becomes an important factor as the depth to length ratio increases. The transverse shear included by the Reissner-Mindlin plate theory offers a better alternative to the Kirchhoff plate theory. Postbuckling analysis of thick composite laminates was considered by [7,8]. Both Kirchhoff thin plate and Mindlin thick plate were analyzed. It indicates that the transverse shear reduces the buckling loads, moreover, the postbuckling stiffness is also reduced by including the transverse shear effects. The major assumption, in the nonlinear range, of both Kirchhoff and Mindlin type plate theories is the

existence of small strains and large in-plane rotations. The independent interpolation of the rotations, in the x and y directions, from the transverse deflection in Mindlin plate theory makes it a difficult task to formulate the governing postbuckling equations. The finite element method of Mindlin type elements offer an attractive method for the solution of postbuckling analysis of laminated plates.

Finally, it is important to notice that various combined experimental and numerical studies were performed to validate the thin laminated plate theory in uniaxial compression over the postbuckling range [9]. To the knowledge of the authors, no biaxial compressive experimental and numerical study was conducted to verify the theory.

3. NONLINEAR CONSTITUTIVE MODELS OF FIBER COMPOSITE LAMINATES

The unusual shear behavior in thermoset fiber composites and matrix nonlinearity in thermoplastic composite systems led to a concern to assess the nonlinear behavior through a suitable formulation of constitutive model and through the examination of such nonlinear effects on the structural responses.

In this chapter, two major theories are reviewed and examined. The first theory considers the stress-strain behavior as a nonlinear elastic. A complementary energy density function is formed and various classes of anisotropic symmetry are imposed on its polynomial basis. The result is a simplified reduced polynomial basis, which a nonlinear constitutive model can be derived from. The second approach used the deformation theory of plasticity and the Ramberg-Osgood characterization of a nonlinear stress-strain relation. These constitutive models are both implemented for the AS4/J polymer composite material.

3.1 Anisotropic Elastic Constitutive Model

3.1.1 Strain Energy and Complementary Energy Density Functions

When given a perfectly elastic body, there exists an elastic strain energy function per unit volume, W, of the undeformed body.

This function is a single-valued function of the strain tensor such that

$$\sigma_{ij} = \frac{1}{2}\left(\frac{\partial W}{\partial e_{ij}} + \frac{\partial W}{\partial e_{ji}}\right) \qquad \text{or} \qquad \sigma_{ij} = \frac{\partial W}{\partial e_{ij}} \tag{1}$$

where $$W = W(e_{ij}) = W(u_{i,j}) \tag{2}$$

The complementary energy density function W* can be defined through

$$W(e_{ij}) + W^*(\sigma_{ij}) = \sigma_{ij}\, e_{ij} \tag{3}$$

It is important to notice that under symmetry operations $\sigma_{ij}\, e_{ij}$ remains invariant. Hence, one can choose a representation of the constitutive model through W or W*.

3.1.2 Polynomial Representation of Strain Energy Function

Assuming that the strain energy function is analytic in its arguments, it can be represented as

$$W(e_{ij}) = \sum_{r=1}^{\infty} W_r(e_{ij}) \tag{4}$$

Where W_r is a homogeneous function of the degree r

$$W_r(\lambda e_{ij}) = \lambda^r W_r(e_{ij}) \tag{5}$$

Obviously it is impossible to consider infinite terms of W_r. Hence, a truncated cubic approximation will be used. It can be written as

$$W = W_o + C_{ij}\, e_{ij} + \frac{1}{2} C_{ijkl}\, e_{ij}\, e_{kl} + \frac{1}{3} C_{ijklmn}\, e_{ij}\, e_{kl}\, e_{mn} \tag{6}$$

Where W_o is an arbitrary constant and C_{ij} is an initial stress tensor. It is easy to notice that a quadratic form of W yields linear constitutive relations.

3.1.3 Material Symmetry

If the anisotropic material is considered to be homogeneous and possesses symmetry due to the fibers positioning, certain restrictions can be imposed on the polynomial basis of W. Given that X_i' and X_i are two equivalent symmetric orientations, one can write

$$W(e_{ij}) = W(e_{ij}') = W(a_{ik}\, a_{jl}\, e_{kl}) \tag{7}$$

and $$a_{ij} = \cos(x_i', x_j)$$

Next, we will define some basic symmetric transformation operators

I -- Identity transformation.

-I -- Inverse transformation.

R_i -- Reflection of the i-th axis, $x_i' = - x_i$.

$S^{i_n,\alpha}$ Right-handed rule rotation through α degrees around the axis in the direction of the normal n.

These symmetric operators will be used to define some basic crystalline systems.

Triclinic System (I, -I)

The identity and inverse transformations do not effect the stress or strain tensors. Hence, there can be no restrictions placed on the polynomial basis of the strain energy function.

$$W(e_{ij}) = W(e_{11}, e_{22}, e_{33}, e_{12}, e_{23}, e_{13}) \tag{8}$$

Monoclinic Symmetry

For material having Monoclinic symmetry, the transformation operators defining this symmetry are

$$I, -I, S^{i_3,\pi} \tag{9}$$

The first two operators do not effect the form of the polynomial basis. The rotation of the cartesian coordinate system in π degrees around the x_3 axis yields

$$e'_{23} = -e_{23} \qquad \text{and} \qquad e'_{13} = -e_{23} \tag{10}$$

Hence, the ..nitation imposed on the form of the strain energy function is

$$W(e_{11}, e_{22}, e_{33}, e_{12}, e_{23}, e_{13}) = W(e_{11}, e_{22}, e_{33}, -e_{23}, -e_{13}) \tag{11}$$

This will create two sets of variables which the polynomial basis is symmetric in

$$(a_1, a_2) = (e_{23}, e_{13}) \qquad \text{and} \qquad (b_1, b_2) = (-e_{23}, -e_{13}) \tag{12}$$

Applying group theorems (1) and (3) in appendix A to produce a polynomial basis for W in the form

$$W = W(J_1, J_2, J_3, J_4, K_1, K_2, K_{11}, K_{12}, K_{22}) \tag{13}$$

Where J_i are the invariant quantities under the above transformation, and

$$K_1 = K_2 = 0$$

$$K_{11} = e_{23}^2, \qquad K_{12} = e_{13}\, e_{23}, \qquad K_{23} = e_{23}^2 \tag{14}$$

The reduced polynomial basis of the strain energy is

$$W = W(e_{11}, e_{22}, e_{33}, e_{12}, e_{13}^2, e_{23}^2, e_{13}\, e_{23}) \tag{15}$$

Orthotropic Symmetry

A material having three mutually orthogonal planes of symmetry is called orthotropic material. The basic symmetry operators are

$$I, -I, S^{i_1,\pi}, S^{i_2,\pi}, S^{i_3,\pi} \tag{16}$$

The first three operators were applied to produce Equation (15), applying the fourth operator yields

$$e'_{12} = -e_{12} \qquad e'_{23} = -e_{23} \tag{17}$$

The symmetry limitation imposed on W in equation (15) will be

$$W(e_{11}, e_{22}, e_{33}, e_{12}, e_{23}^2, e_{13}^2, e_{13}\, e_{23}) =$$

$$W(e_{11}, e_{22}, e_{33}, -e_{12}, e_{23}^2, e_{13}^2, -e_{13}\, e_{23}) \tag{18}$$

We can identify two sets of variables which the polynomial basis is symmetric in

$$(a_1, a_2) = (e_{12}, e_{13}\, e_{23}) \text{ and } (b_1, b_2) = (-e_{12}, -e_{13}\, e_{23}) \tag{19}$$

Using group thecrems (1) and (3) in appendix A, the polynomial basis of W is

$$W = W(J_1, J_2, J_3, J_4, J_5, K_1, K_2, K_{11}, K_{12}, K_{22}) \tag{20}$$

Where J_i are the transformation invariants, writing K_i and K_{ij}

$$K_1 = K_2 = 0$$

$$K_{11} = e_{12}^2, \qquad K_{12} = e_{12}e_{13}e_{23}, \qquad K_{22} = e_{13}^2e_{23}^2 \tag{21}$$

Hence,

$$W = W(e_{11}, e_{22}, e_{33}, e_{12}^2, e_{23}^2, e_{13}^2, e_{12}e_{13}e_{23}) \tag{22}$$

Applying $S^{i_1,\pi}$ will not effect the form of W because if there are two orthogonal symmetric planes the third orthogonal plane is also symmetric.

Transverse Isotropy

A composite unidirectional fibrous reinforced material aligned in x_3 direction, in which the x_1 x_2 plane is compsoed of a hexagonal or random array of fibers, is said to have a transverse isotropic symmetry. The basic symmetric operators are

$$I, -I, R_1, S^{i_3,\alpha} \qquad (\alpha \text{ - arbitrary}) \tag{23}$$

For an arbitrary rotation of the coordinate system around x_3 axis, the new coordinate system can be expressed as

$$X_i' = a_{ij} X_j \tag{24}$$

An alternative representation of (24) is

$$X_1^1 + iX_2^1 = e^{-i\alpha} (X_1 + iX_2), \qquad X_3^1 = X_3 \tag{25}$$

Can show

$$\begin{aligned} e_{11}' + e_{22}' &= e_{11} + e_{22} \\ e_{33}' &= e_{33} \\ e_{11}' - e_{22}' + 2ie_{12}' &= e^{-2i\alpha} (e_{11} - e_{22} + 2i\, e_{12}) \\ e_{13}' + ie_{23}' &= e^{-i\alpha} (e_{13} + ie_{23}) \end{aligned} \tag{26}$$

We can identify the following invariants

$$J_1 = e_{11} + e_{22} \qquad J_2 = e_{31}^2 + e_{23}^2 \qquad J_3 = e_{33} \tag{27}$$

If we define the quantities

$$E_1 = e_{11} - e_{22} \qquad F_1 = e_{13}^2 - e_{23}^2$$
$$E_2 = 2e_{12} \qquad F_2 = 2\, e_{13}\, e_{23} \tag{28}$$

From the transformation, can show

$$\begin{aligned} E_1' &= E_1 \cos 2\alpha + E_2 \sin 2\alpha \\ E_2' &= E_2 \cos 2\alpha - E_1 \sin 2\alpha \\ F_1' &= F_1 \cos 2\alpha + F_2 \sin 2\alpha \\ F_2' &= F_2 \cos 2\alpha - F_1 \sin 2\alpha \end{aligned} \tag{29}$$

Symmetry requirement imposed on the form of W, can be stated as

$$W(J_1, J_2, J_3, E_1, E_2, F_1, F_2) = W(J_1, J_2, J_3, E_1', E_2', F_1', F_2') \tag{30}$$

Applying group theorem (2) in Appendix A, where the vectors $\alpha_i^{(1)}$ and $\alpha_i^{(2)}$ are

$$\alpha_i^{(1)} = (E_1, E_2) \qquad \alpha_i^{(2)} = (F_1, F_2) \qquad n = 2 \tag{31}$$

The invariant forms due to the above orthogonal transformation are

$$\alpha_i^{(1)}\alpha_i^{(1)} = E_2^2 + E_2^2 = J_1 - 4J_4$$

$$\alpha_i^{(1)}\alpha_i^{(2)} = E_1F_1 + E_2F_2 = J_2^2 \qquad (32)$$

$$\alpha_i^{(2)}\alpha_i^{(2)} = F_2^1 + F_2^2 = 2J_5 + J_1J_2 - 2J_3J_4$$

$$\Delta = E_1F_2 - E_2F_1$$

Where J_1, J_2, J_3 are defined in (27) and

$$J_4 = e_{11}\, e_{22} - e_{12}^2$$

$$J_5 = |e_{ij}| \qquad (33)$$

W can be expressed in the polynomial basis as

$$W = W(J_1, J_2, J_3, J_4, J_5) \qquad (34)$$

Assumptions and Simplifications

Consider a transversely isotropic material where x_1 coincides with the fibers direction. If the given lamina is to be considered in a state of plane stress, the form of W will be considerably simplified as

$$W = W(e_{11}, e_{22}, e_{12}^2) \qquad (35)$$

The same argument can be made with the complementary stress energy density function, using the relation (3)

$$W^* = W^*(\sigma_1, \sigma_2, \sigma_6^2) \tag{36}$$

An approximated fourth degree of W^* can be written as

$$\begin{aligned} W^* = {} & \frac{1}{2} S_{11}\sigma_1^2 + \frac{1}{2} S_{22} \sigma_2^2 + S_{12} \sigma_1 \sigma_2 + \frac{1}{2} S_{66} \sigma_6^2 + \\ & \frac{1}{3} S_{111} \sigma_1^3 + \frac{1}{3} S_{222} \sigma_2^3 + S_{112} \sigma_1^2 \sigma_2 + S_{122} \sigma_1 \sigma_2^2 + \\ & S_{166} \sigma_1 \sigma_6^2 + S_{266} \sigma_2 \sigma_6^2 + \frac{1}{4} S_{1111} \sigma_1^4 + \frac{1}{4} S_{2222}\sigma_2^4 + \\ & \frac{1}{4} S_{6666} \sigma_6^4 + S_{1112} \sigma_1^3 \sigma_2 + S_{1122} \sigma_1^2 \sigma_2^2 + \\ & S_{1222} \sigma_1 \sigma_2^3 + S_{1166} \sigma_1^2 \sigma_6^2 + S_{2266} \sigma_2^2 \sigma_6^2 + S_{1266} \sigma_1 \sigma_2 \sigma_6^2 \end{aligned} \tag{37}$$

According to Hahn and Tsai [4], the interaction terms between σ_1 and σ_6 or σ_2 and σ_6 are neglected for the material they experimented with. It has been shown that an important effect is produced on the resolved transverse stress in a uniaxial test for a wide range of fiber orientations. Hence, the only effect considered by their model was the effect of shear stress nonlinearity without any interaction terms which may involve other stress components in the form of W^*.

Finally, the complementary energy density function is reduced to

$$W^* = \frac{1}{2} S_{11} \sigma_1^2 + \frac{1}{2} S_{22} \sigma_2^2 + S_{12} \sigma_1 \sigma_2 + \frac{1}{2} S_{66} \sigma_6^2 + \frac{1}{4} S_{6666} \sigma_6^4 \qquad (38)$$

Note that the shear components appear separately in their powers and that there are no interaction terms. Also, the only nonlinearity is in the axial shear. The constitutive stress-strain relations can be derived from

$$e_{ij} = \frac{\partial W^*}{\partial \sigma_{ij}} \qquad (39)$$

3.2 Deformation Theory and Ramberg-Osgood Representation

Deformation type nonlinear stress-strain relations can be represented in the form

$$e_{ij} = S_{ijkl} \sigma_{kl} \qquad (40)$$

Where S_{ijkl} is a function of the average stresses or the proper stress invariants. If the material is transversely isotropic, and the fibers are alligned in the x_1 direction, the stress invariants are obtained in Equations (27) and (33). It is convenient to express the strain tensor into a linear elastic part e_{ij}^e and a nonlinear strain part e_{ij}^p such that

$$e_{ij} = e^{e}_{ij} + e^{p}_{ij} \tag{41}$$

it follows

$$S_{ijkl} = S^{e}_{ijkl} + S^{p}_{ijkl} \tag{42}$$

where

$$S^{p}_{ijkl} = S^{p}_{ijkl}(J_1, J_2, J_3, J_4, J_5) \tag{43}$$

Consider a thin lamina in a state of plane stress, the effective nonlinear compliances are a function of the three average plane-stress components

$$S^{P}_{ijkl} = S^{P}_{ijkl}(\sigma_{11}\sigma_{22}\sigma^{2}_{12}) \tag{44}$$

The nonlinear stress-strain relations are

$$\begin{aligned} e^{P}_{11} &= S^{P}_{11}\,\sigma_{11} + S^{P}_{12}\,\sigma_{22} \\ e^{P}_{22} &= S^{P}_{12}\,\sigma_{11} + S^{P}_{22}\sigma_{22} \\ e^{P}_{12} &= S^{P}_{66}\,\sigma_{12} \end{aligned} \tag{45}$$

For unidirectional fiberous reinforced materials, the fibers direction is clearly stiffer than the matrix. Therefore, the average stress σ_{11} can be assumed to be carried by the fibers. The other

stress components σ_{22} and σ_{12} are carried by the matrix and give the nonlinear behavior. The only nonlinear parts of the compliance tensor are

$$S_{22}^P = S_{22}^P(\sigma_{22},\sigma_{12}^2) \quad \text{and} \quad S_{66}^P = S_{66}^P(\sigma_{22},\sigma_{12}^2) \tag{46}$$

Next, one dimensional representation of nonlinear stress-strain relations in Ramberg-Osgood form are

$$\begin{aligned} e_{22} &= e_{22}^e + e_{22}^P = \frac{\sigma_{22}}{E_2}\left[1 + \left(\frac{\sigma_{22}}{\sigma_Y}\right)^{M-1}\right] \\ e_{12} &= e_{12}^e + e_{12}^P = \frac{\sigma_{12}}{G_{12}}\left[1 + \left(\frac{\sigma_{12}}{\tau_Y}\right)^{N-1}\right] \end{aligned} \tag{47}$$

Where E_2 is the transverse elastic Young's modulus and G_{12} is the axial elastic shear modulus. The parameters σ_Y τ_Y, M,N are curve fitting parameters.

3.2.1 J_2 - Deformation Theory

The basic assumption of the deformation theory of plasticity, for isotropic materials, is that the plastic strains can be represented as

$$e_{ij}^P = f(J_2)\, S_{ij} \tag{48}$$

Where S_{ij} is the deviatoric stress and J_2 is its second invariant

$$S_{ij} = \sigma_{ij} - \frac{1}{3}\sigma_{kk}\delta_{ij}$$

$$J_2 = \frac{1}{2} S_{ij}S_{ij} \tag{49}$$

Similarly, we can generalize this to anisotropic materials by assuming that

$$e_{ij}^{P} = f(L)\, S_{ij} \tag{50}$$

Where L is a general quadratic function of the stress invariants. Consider a state of plane stress, the invariant forms resulting from symmetry consideration are

$$\sigma_{11}, \sigma_{22}, \sigma_{12}^2 \tag{51}$$

Assuming that the stress σ_{11} does not produce any plastic strain since it is mainly carried by the fibers, L is a quadratic function of σ_{22} and σ_{12}^2

$$L = L(\sigma_{22},\sigma_{12}^2) = \alpha^2\sigma_{22}^2 + \beta^2\sigma_{12}^2 \tag{52}$$

Note that there is nothing fundamental in the assumption of the general quadratic form in Equation (50). Next, we can determine the coefficients α, β from a comparison of the nonlinear one dimensional stress-strain relations with the Ramberg-Osgood stress-strain representation.

A Ramberg-Osgood representation of one dimensional transverse stress

$$e_{22}^P = S_{22}^P(\sigma_{22})\,\sigma_{22} = \frac{\sigma_{22}}{E_2}\left[\left(\frac{\sigma_{22}}{\sigma_Y}\right)\right]^{M-1} \tag{53}$$

or

$$e_{22}^P = \frac{\sigma_{22}}{E_2}\left[\left(\frac{\sigma_{22}}{\sigma_Y}\right)^2\right]^{\frac{M-1}{2}} \tag{54}$$

From the deformation theory, the nonlinear part of the transverse strain is

$$e_{22}^P = \frac{\sigma_{22}}{E_2} f_{22}(L) = \frac{\sigma_{22}}{E_2} f_{22}(\alpha^2\,\sigma_{22}^2) \tag{55}$$

Comparing Equations (54) and (55) leads to

$$\alpha^2 = \frac{1}{\sigma_Y^2} \quad \text{and} \quad f_{22} = L^{\frac{M-1}{2}} \tag{56}$$

The function f_{22} is the quadratic form L to the (M-1)/2 power.

Similarly, in the case of one dimensional σ_{12}, the nonlinear strain in the Ramberg-Osgood form is

$$e_{12}^P = S_{66}^P(\sigma_{12}^2)\,\sigma_{12} = \frac{\sigma_{12}}{G_{12}}\left[\left(\frac{\sigma_{12}}{\tau_Y}\right)^2\right]^{\frac{N-1}{2}} \tag{57}$$

From the deformation theory, the nonlinear shear strain is

$$e_{12}^P = \frac{\sigma_{12}}{G_{12}} f_{66}(L) = \frac{\sigma_{12}}{G_{12}} f_{66}\left(\beta^2 \sigma_{12}^2\right) \tag{58}$$

Comparing Equations (57) and (58), it follows that

$$\beta^2 = \frac{1}{\tau_Y^2} \qquad \text{and} \qquad f_{66} = L^{\frac{N-1}{2}} \tag{59}$$

Finally, the nonlinear compliances can be expressed as

$$S_{22}^P = \frac{1}{E_2}\left[(\alpha\sigma_{22})^2 + (\beta\sigma_{12})^2 \right]^{\frac{M-1}{2}}$$

$$S_{66}^P = \frac{1}{G_{12}}\left[(\alpha\sigma_{22})^2 + (\beta\sigma_{12})^2 \right]^{\frac{N-1}{2}} \tag{60}$$

where

$$\alpha^2 = \frac{1}{\sigma_Y^2} \qquad \beta^2 = \frac{1}{\tau_Y^2}$$

The parameters σ_Y, M and τ_Y,N respectively are curve fitting parameters for the Ramberg-Osgood representation of stress-strain curves in a one dimensional case.

It follows that the nonlinear plane stress-strain relations are

$$e_{11} = \frac{1}{E_1}\sigma_{11} - \frac{\vartheta_{12}}{E_1}\sigma_{22}$$

$$e_{22} = -\frac{\vartheta_{12}}{E_1}\sigma_{11} + \frac{\sigma_{22}}{E_2}\left\{1+\left[\left(\frac{\sigma_{22}}{\sigma_Y}\right)^2 + \left(\frac{\sigma_{12}}{\tau_Y}\right)^2\right]^{\frac{M-1}{2}}\right\} \tag{61}$$

$$e_{12} = -\frac{\sigma_{12}}{G_{12}}\left\{1+\left[\left(\frac{\sigma_{22}}{\sigma_Y}\right)^2 + \left(\frac{\sigma_{12}}{\tau_Y}\right)^2\right]^{\frac{N-1}{2}}\right\}$$

4. FINITE ELEMENT FORMULATIONS

The objective of this chapter is to describe the finite element method used to solve nonlinear structural systems. The well known virtual work principal is used as a 'weak form' to derive the equilibrium equations

$$\int_v B^T \sigma \, dv - P = 0 \tag{62}$$

Where P is the applied force vector, B is the strain-displacement matrix assembled in the global structural coordinates along with the stress vector. Equation (62) can be written as

$$I(u) = P \tag{63}$$

Where I is the internal resisting force vector and is a nonlinear function of the nodal displacements in the case of nonlinear geometric problems. The representation of the virtual work expression in Equation (63) can lead to two basic finite element formulations. The first is the secant stiffness matrix formulation which relates the total displacement with the total load vector. The second method is an incremental formulation which defines a relation between increments of loads and displacements through a tangent stiffness matrix. This method can be derived by differentiating Equation (63), it follows that

$$K_t \Delta U = \Delta p \tag{64}$$

where

$$K_t = K_o + (K_1 + K_1^T + K_2) + K_G$$

$$K_o = \int_v B_l^T C B_l dv$$

$$K_1 = \int_v B_l^T C B_{nl} dv \tag{65}$$

$$K_2 = \int_v B_{nl}^T C B_{nl} dv$$

$$K_G = \int_v G^T M_\sigma G dv$$

Note that the matrix K_1 is nonsymmetric and is a linear function in the nodal displacements. K_o is a constant independent matrix. The quantity in parenthesis is called the initial displacement matrix and is symmetric. Different combined incremental-iterative techniques are used to solve the nonlinear set of algebraic equations (64). The Newton-Raphson (NR) and its modifications are the most known and used methods. These methods can be described as

$$K_t \ \Delta U_{n+1}^{i+1} = P_{n+1} - I_{n+1}^i \tag{66}$$

Where i is the iteration number and n is the step or increment number. The internal resistance vector I_{n+1}^i is updated according to the method used.

The load increment P_{n+1} is specified for a fixed load level method, whereas, in the case of variable NR iterative methods, the load increment P_{n+1} is part of the solution. These methods follow the structure equilibrium path of a structure initially subject to a given load pattern P_o in the form

$$P = \lambda P_o \tag{67}$$

were λ is a scalar determined by adding a constraint to the equilibrium equations.

In order to accurately simulate the decrease in the load and displacement near limit or bifureation points, where the tangent stiffness becomes singular, a modified-Riks (11) iterative algorithm is used to follow the equilibrium path. The basic idea of the Riks method is moving along the tangent line to the equilibrium path and searching for an equilibrium point located in the plane orthogonal to the tangent line.

This study makes use of the ABAQUS finite element code (12) where the modified Riks method is implemented. The nonlinear formation is the updated Lagrangian method in which the reference configuration is updated to an intermediate configuration between the original and current configurations. Thus, the current and reference configurations remain close.

4.1. Element Formulation

The plate element used in the postbuckling analysis is the isoparametric 8-nodes quadrilateral plate element. It has six degrees of freedom (D.O.F.) in each node which includes three displacements and three rotations. The element is based on the Reissner-Mindlin plate theory. Numerical formulations are more simple and convenient to implement than the Kirchhoff plate elements. The theory also accommodates for transverse shear strains. The continuity requirement is C^o continuity due to the fact that only first order derivatives of the D.O.F. appear in the virtual work expressions. The displacements and rotations are decoupled. Hence, the element is mappable and allows modeling of complex geometries.

The displacement field is

$$u(x,y,z) = u^o(x,y) - Z\theta_x$$

$$v(x,y,z) = v^o(x,y) - Z\theta_y \qquad (68)$$

$$w(x,y,z) = w(x,y)$$

The above displacement field is independently interpolated within the element

$$u^o = N_i U_i \qquad V^o = N_i V_i \qquad W = N_i W_i$$

$$\theta_x = N_i \theta_{xi} \qquad \theta_y = N_i \theta_{yi} \qquad (69)$$

The notation used is the index summation on the element nodes. The nonlinear strain-displacement relations, defined in appendix B, are applied to the displacement field in (68) and yield

$$\varepsilon_{xx} = u^{o}_{,x} + \frac{1}{2} w^{2}_{,x} - Z\,\theta_x$$

$$\varepsilon_{yy} = v^{o}_{,y} + \frac{1}{2} w^{2}_{,y} - Z\,\theta_y$$

$$\varepsilon_{xy} = u^{o}_{,y} + v^{o}_{,x} + w_{,x} w_{,y} - Z\,\theta_{x,y} - Z\theta_{y,x} \qquad (70)$$

$$\varepsilon_{xz} = w_{,x} - \theta_x\, y$$

$$\varepsilon_{yz} = w_{,y} - \theta_y$$

Both Equations (69) and (70) defines the strain-displacement matrix B in the form

$$\begin{bmatrix} \delta\varepsilon_{xx} \\ \delta\varepsilon_{yy} \\ \delta\varepsilon_{xy} \\ \delta\varepsilon_{xz} \\ \delta\varepsilon_{yz} \end{bmatrix} = \left[\begin{bmatrix} N_{i,x} & 0 & 0 & -ZN_{i,x} & 0 \\ 0 & N_{i,y} & 0 & 0 & -ZN_{i,y} \\ N_{i,y} & N_{i,x} & 0 & -ZN_{i,y} & -ZN_{i,x} \\ 0 & 0 & N_{i,x} & -N_i & 0 \\ 0 & 0 & N_{i,y} & 0 & -N_i \end{bmatrix} + \right. \qquad (71)$$

$$\left. \begin{bmatrix} 0 & 0 & W_j N_{j,x} N_{i,x} & 0 & 0 \\ 0 & 0 & W_j N_{j,y} N_{i,y} & 0 & 0 \\ & & W_j N_{j,y} N_{i,x+} & & \\ 0 & 0 & W_j N_{j,x} N_{i,y} & 0 & 0 \\ 0 & 0 & 0 & 0 & 0 \\ 0 & 0 & 0 & 0 & 0 \end{bmatrix} \right] \begin{bmatrix} \delta U_i \\ \delta V_i \\ \\ \delta W_i \\ \delta\theta_{xi} \\ \delta\theta_{yi} \end{bmatrix}$$

Equation (71) defines linear and nonlinear parts of the strain-displacement matrix. Again, note the summation over indices i and j where they represent the element nodes.

4.2 Constitutive Tangent Stiffness

The material tangent stiffness or Jacobian matrix of the constitutive model relates incremental stresses and strains. It can be defined as

$$C_{ij} = \frac{\delta \Delta \sigma_i}{\delta \Delta \varepsilon_i} \tag{72}$$

Where $\Delta\sigma_i$ and $\Delta\varepsilon_j$ are the stress and strain incremental vectors. In the case of material and geometric nonlinearities, the material model should be formed in an incremental form to accommodate with the incremental finite element formulations.

Three constitutive models are considered in this study. The first model, presented in Chapter 3, considers the axial shear nonlinearity. The incremental form of this model, in a plane-stress condition, is

$$\begin{Bmatrix} de_1 \\ de_2 \\ de_6 \end{Bmatrix} = \begin{bmatrix} S_{11} & S_{12} & 0 \\ S_{12} & S_{22} & 0 \\ 0 & 0 & S_{66} + 3S_{6666}\sigma_6^2 \end{bmatrix} \begin{Bmatrix} d\sigma_1 \\ d\sigma_2 \\ d\sigma_6 \end{Bmatrix} \tag{73}$$

The second model considers uncoupled transverse and shear stress-strain relations. Its incremental form is

$$\begin{Bmatrix} de_1 \\ de_2 \\ de_6 \end{Bmatrix} = \begin{bmatrix} S_{11} & S_{12} & 0 \\ S_{12} & S_{22} + 3S_{2222}\sigma_2^2 & 0 \\ 0 & 0 & S_{66} + 3S_{6666}\sigma_6^2 \end{bmatrix} \begin{Bmatrix} d\sigma_1 \\ d\sigma_2 \\ d\sigma_6 \end{Bmatrix} \tag{74}$$

The third model considered in 3.1.4 for coupled transverse and shear stress-strain in Ramberg-Osgood representation. The incremental form for this model, in the case of M=N=3, is

$$\begin{Bmatrix} de_1 \\ de_2 \\ de_6 \end{Bmatrix} = \begin{bmatrix} S_{11} & S_{12} & 0 \\ S_{12} & S_{22}\left(1 + 3\alpha^2\sigma_2^2 + \beta^2\sigma_6^2\right) & 2S_{22}\beta^2\sigma_2\sigma_6 \\ 0 & 2S_{66}\alpha^2\sigma_2\sigma_6 & S_{66}\left(1 + \alpha^2\sigma_2^2 + \beta^2\sigma_6^2\right) \end{bmatrix} \begin{Bmatrix} d\sigma_1 \\ d\sigma_2 \\ d\sigma_6 \end{Bmatrix} \tag{75}$$

The Jacobian matrix of this model is not symmetric. This will invoke unsymmetric equation solves. All these models are in the materials coordinate system and need to be transformed in the global structural coordinates for each layer. The relation for the transverse stress-strain is considered linear and introduced to the formulation through shear correction factors.

The material considered in this study is AS4/J_1 polymer composite. The stress-strain curves are presented in Fig. 2 and Fig. 3.

4.3 Imperfection Analysis

In order to generate a solution for plates in the postbuckling range and to enable the plate to deform in the transverse direction due to inplane forces, an imperfection technique is implemented in the finite element model. This method is carried out by either a perturbation of the model nodes in the transverse direction such that it will include some of the first eigen vectors in its form, or by applying small distributed loads in the transverse direction at the beginning of the analysis.

5. NUMERICAL RESULTS

5.1 Plate Geometry and Boundary Conditions

This study considers the problem of buckling and postbuckling analysis of laminated plates. The material constitutive models developed in Chapter 3 are implemented in an incremental nonlinear finite element formulation. The plates have a square geometry (L = 300mm) and are subjected to a compressive biaxial in-plane loading. The laminate stack sequence considered is a quasi-isotropic laminate $[0/90/\pm45]_{ns}$. The plate edges are constrained to produce a uniform displacement in the x and y direction respectively. Both in the buckling and postbuckling analysis a full finite element mesh is used due to the nonlinear geometry involved. Most of the results are presented in the form of the applied load, normalized by the plate critical load, versus end-shortening in the x direction, normalized by the plate thickness. The effect of stress-biaxiality ratio is studied for a clamped plate with different aspect-ratios (t/L = 0.02, 0.04, 0.08). The range of biaxial loading ratios are chosen for the values: 0, 0.5, 1.,2. . For $N_y/N_x = 0$. this is the case of uniaxial loading.

5.2 Linearized Buckling and Imperfection Analysis

In order to enable the plate to deform in the lateral direction due to membrane forces, a geometric imperfection is introduced in the finite element mesh. The first three eigenmodes, derived from

linearized buckling analysis, are combined in a linear combination and scaled by some percentage of the plate thickness. It is a well known fact that plate structures are not sensitive to the form of imperfection. Nevertheless, a smaller percentage of imperfection implemented, the more the postbuckling response is close to the real behavior. One percent of the thickness is chosen to scale the linear combination of the first three eigenmodes. This will enable the plate response to be very close to the real perfect structure.

5.3 Materials Models

The fiber reinforced material considered in this study is made of AS4/J1 thermoplastic matrix. The effective elastic properties of this composite system are:

$$E_{11} = 17.9 \times 10^6 \text{ psi}, \quad E_{22} = 0.9 \times 10^6 \text{ psi}, \quad \vartheta_{12} = 0.313$$
$$G_{12} = G_{13} = 0.77 \times 10^6 \text{ psi}, \quad G_{23} = 0.31 \times 10^6 \text{ psi}$$

The nonlinear stress-strain curves for this material, in axial shear [13] and transverse tensile-compression, are presented in figs. 2-3. The three nonlinear constitutive models developed in Chapter 3 are formulated based on these one-dimensional stress-strain curves. These models are referred to as model 1, 2 and 3 in the following discussions.

5.4 Convergence Study

The convergence rate, in finite element analysis of plates, depends strongly upon the plate aspect-ratio (t/L). A large number of elements are required to obtain an accurate solution for thick laminates, especially in the postbuckling range. Hence, the case study chosen is a clamped plate under biaxial compressior (N_y/N_x = 0.5) with an aspect-ratio of 0.08. Fig. 4 illustrates the rate of convergence in the prebuckling and postbuckling ranges for n x n element mesh refinement. Based on these results, the 8 x 8 elements mesh was chosen in the following analysis. It should be noted at this stage that there is an enormous amount of computational time needed for the postbuckling analysis where the material model is nonlinear. A typical 8 x 8 isoparametric 8-nodes quadrilateral shell elements modeling a $[0/90/\pm45]_{5s}$ laminated plate require a large number of Gaussian integration points (2 x 2 x 64 x 40 Gaussian points). This calculation assumes that each lamina is modeled through the thickness with one integration point. The material model would be called about 10,000 times per one iteration! Noting that a typical postbuckling analysis requires hundreds of iterations, one can clearly realize the large amount of computational time involved. Hence, the stack sequence chosen for most of this study was $[0/90/\pm45]_s$. A design of thick laminates requires the use of a sublaminate technique whereby a typical repeating sublaminate includes the material nonlinearities.

5.5 Effect of Thickness

The laminate aspect-ratio effect on the postbuckling behavior is studied for $[0/90/\pm45]_{ns}$ clamped plate under biaxial compression (N_y/N_x = 0, 0.5,.1., 2.). The thickness/length ratios considered are: 0.02, 0.04, 0.08. Figs. 5-8 illustrates the end-shortening curves of three laminates with different aspect-ratio and different biaxial loading. It is shown that the postbuckling stiffness decreases, as the load increases, for large aspect-ratio (t/L = 0.08). This is due to the growing effect of transverse shear in thick plates. The first nonlinear material model is plotted along each curve. The nonlinear curves of plate response with aspect-ratio less than 0.04 do not show a difference compared to the linear material response. Note the early separation of the linear and nonlinear curves for t/L = 0.08. This indicates that there is a difference in the buckling load between the two models. This shift or separation of curves shows that the nonlinear plate is more flexible. This flexibility is expressed by looking at a fixed load level and considering that the corresponding difference of the displacement is much higher than the difference in the load for a fixed value of the displacement.

It can be concluded that the more the postbuckling stiffness is decreasing, the more the effect of material nonlinearities can be seen. Also, the nonlinear response is associated with large deflections. The only nonlinear material model considered in the above figures is the first model which includes the axial shear nonlinearity. The other models are considered in the following figures for t/L = 0.08.

5.6 Thick-Section Plates

The three nonlinear models are considered in the analysis of a thick-section plate (t/L = 0.08) with biaxial loading (N_y/N_x = 0/ 0.5, 1, 2) and stack sequence $[0/90/\pm45]_s$. The end-shortening of the plate versus the normalized applied load is presented in figs. 9-11. The plate center deflection is presented in figs. 13 '5. These figures clearly demonstrate the effect of nonlinear behavior of fiber composite materials upon the global response of the structure. The closest nonlinear behavior to the linear response is the nonlinear axial shear model (model 1). Model 2 and 3 follow in order. This consistent pattern of behavior can be explained by the fact that model 2 includes the transverse nonlinear response along with the nonlinear in-plane shear, in an independent fashion. Model 3 considers both nonlinearities along with interaction terms. It can be expected that model 3 produces the largest nonlinear effect. The same conclusion can be drawn from the lateral deflection curves figs. 13-15 for different biaxial loading ratios.

Finally, an additional case of multi-layered thick laminate $[0/90/\pm45]_{12s}$ is considered. The aspect ratio in (t/L = 0.08) and the biaxial loading ratio is N_y/N_x = 1. . The end-shortening postbuckling response is presented in fig. 16. the lateral displacement behavior is presented in fig. 17. Both curves indicate that the three nonlinear models produce a very close response in most of the postbuckling range. This behavior can be explained by the presence of large

number of layers of 0° and 90° degree fiber angles. These layers carry most of the applied loads in the fiber directions. As a result, the nonlinear strain distribution in the matrix is reduced. Figs. 18-19 support this observation. In these figures the transverse shear-stress resultants V_x and V_y are presented respectively. The location of these resultants is the mid-point of the upper right quarter of the plate. These figures indicate that the nonlinear models do not affect the stress distribution in the structure as much as producing relatively large displacements. Also, fig. 20 shows the strain in the fiber direction of the upper and lower layers at the plate center. It is shown that the strain in the fiber direction can be considered as a linear elastic strain with no plastic or nonlinear part.

6. CONCLUDING REMARKS

The approach utilized in this report was to present two major theories of nonlinear constitutive models of stress-strain behavior. The first approach considers the stress-strain as nonlinear elastic relations, which are derived through the use of a complementary energy density function and takes into account the material symmetries. The second approach was to adopt the Ramberg-Osgood representation of the one-dimensional nonlinear stress-strain curves. By utilizing the deformation theory as a representation of the nonlinear parts of the strain, a nonlinear stress-strain behavior was obtained. The first two models, referred as model 1 and model 2, are based on the first approach. Model 1 represents the nonlinear axial shear behavior. In addition, model 2 takes into account the transverse stress-strain behavior in an independent fashion. The third model is based on the second approach of deformation theory. It includes both nonlinear stress-strain relations. Moreover, an interaction expression was formulated to account for simultaneous presence of axial shear and transverse stress.

The postbuckling results of thick section laminated plates indicates that the nonlinear stress-strain behavior has a global effect on the structural response. The stiffness was reduced and a large displacement was associated with the structural behavior. The distribution of the stress resultant in plate seems not to have a major change compared to the linear response.

It is important to emphasize that the problems analyzed in this study do not include any stress singularities such as matrix cracking, delamination, holes and cutouts. These local effects can have a significant inelastic behavior. The question of the effect of nonlinear constitutive behavior on such local damage modes and structural discontinuities should be addressed as a continuation of this study.

A comparison of the three models presented yields that the first model produces the most conservative response. The interaction terms in the deformation theory model gives a difference of response than the other models. The structural behavior of multi-layered thick laminates which are associated with these constitutive models are very close. This result indicates that the presence of large numbers of unidirectional layers oriented in different directions decreases the nonlinear strains by the fact that the fiber direction can carry most of the applied loads.

Failure criterias were not used in this study. Obviously, the laminated thick section plate will be damaged in the process of postbuckling or even prebuckling response. Hence, it is important to include failure and local effects in a future study.

APPENDIX A

The following short review covers three mathematical group theorems. Mathematical discussion and proofs are beyond the context of this study and can be found in [10].

Theorem (1)

A polynomial basis for polynomials, which are symmetric in the two sets of variables $(a_1, a_2, ..., a_n)$ and $(b_1, b_2, ..., b_n)$, is formed from the quantities

$$K_j = \frac{1}{2}(a_j + b_j)$$

$$K_{jk} = \frac{1}{2}(a_j b_k + a_k b_j) \qquad j,k = 1,2,...,n$$

Theorem (2)

A polynomial basis for polynomials, which are symmetric in the n vectors $\alpha^{(r)} = (\alpha_1, \alpha_2, ..., \alpha_n)^{(r)}$ in n-dimensional space, and which is invariant under all proper orthogonal transformations, is formed by the scalar products

$$\alpha_i^{(r)} \alpha_i^{(s)}$$

and

$$|\alpha_s^{(r)}| \qquad i,r,s = 1,2,...,n$$

Theorem (3)

A polynomial basis for a polynomial in the variables $(a_1,a_2,...,a_n)$, $(b_1,b_2,...,b_n)$ and $(J_1,J_2,...,J_k)$, which is form-invariant under a group of transformations and $(J_1,J_2,...,J_k)$ are invariants, is formed by adjoining to the quantities $(J_1,J_2,...,J_k)$ the polynomials in the variables $(a_1,a_2,...,a_n)$ and $(b_1,b_2,...,b_n)$ which are form-invariant under the given group of transformations.

APPENDIX B

Postbucking Analysis of Thin Plates

The purpose of the present appendix is to develop the governing equations for postbuckling analysis of laminated thin plates. Although in this study the postbuckling analysis was performed through the use of the finite element method and for thick and thin plates, it is important to recognize the formulation of the governing equations for postbuckling analysis and that there are different ways to obtain approximated solutions, such as the finite difference method or by a truncated double fourier series method.

In attempting to write the equilibrium equations for postbuckling of plates, one should write the equilibrium equations in the current configuration. By transforming these equations to the original or reference configuration, a set of nonlinear equilibrium equations can be obtained.

A point occupying the reference configuration is denoted as a position vector x, this vector corresponds to the position vector $\bar{x}$ in the deformed configuration, where

$$\overline{X_i} = X_i + u_i \qquad (1)$$

Where u_i is the displacement vector. The deformation gradient tensor is defined as

$$F_{ij} = \frac{\partial \overline{x_i}}{\partial x_j} = \delta_{ij} + u_{i,j} \qquad (2)$$

The Green strain tensor can be written as

$$\varepsilon_{ij} = \frac{1}{2}(F_{ki}F_{kj} - \delta_{ij}) = \frac{1}{2}(u_{i,j} + u_{j,i} + u_{k,i}u_{k,j}) \tag{3}$$

Equilibrium in the deformed configuration, with no body forces, can be expressed as

$$\int_{\bar{s}} \overline{T_i}\, d\bar{s} = 0 \tag{4}$$

Where $\overline{T_i}$ and $d\bar{s}$ are traction vector and element area respectively in the deformed configuration. The stress measure used is the symmetric second Piola-Kirchhoff stress which is obtained by mapping the force transmitted over an element area $d\bar{s}$ in the current configuration to the *reference* configuration

$$\overline{T_i\, d\bar{s}} = F_{ij}\, T_j\, ds = F_{ij}\, \sigma_{jk}\, n_k\, ds \tag{5}$$

Where T_j is a fictitious stress vector acting over an element area ds, with a unit outward normal n_k, in the original configuration. Substituting Equation (5) into (4) yields

$$\int_s F_{ij}\, \sigma_{jk}\, ds = 0 \tag{6}$$

Using the divergence theorem

$$\int_v (F_{ij}\sigma_{jk})_{,k}\, dv = 0 \tag{7}$$

Equation (7) is true for any volume v. The equilibrium equations are

$$[F_{ij}\sigma_{jk}]_{,k} = [(\delta_{ij} + u_{i,j})\sigma_{jk}]_{,k} = 0 \qquad (8)$$

$$i = 1,2,3$$

substituting

$$u_{i,j} = e_{ij} + w_{ij} \qquad (9)$$

Where e_{ij} is the linear engineering strain and w_{ij} is the skew-symmetric rotation-tensor

$$[(\delta_{ij} + e_{ij} + w_{ij})\sigma_{jk}]_{,k} = 0 \qquad (10)$$

Next, we will use the kinimatic assumptions of nonlinear deformation of thin plates, which are known as the von Kármán theory of plates. This theory assumes that the strains can be neglected compared with the rotations. Moreover, for flat thin plates we can neglect the rotation w_{12}. Introducing these assumptions in Equation (10)

$$[(\delta_{ij} + w_{ij})\sigma_{jk}]_{,k} = 0 \qquad i = 1,2,3 \qquad (11)$$

Writing the set of Equations (11) explicitly, we can show that the first tow equations, i = 1,2, are reduced to the well known linear equilibrium equations. The only nonlinear equation is the equilibrium equation in the Z direction

$$\sigma_{\alpha\beta,\beta} = 0 \qquad \alpha,\beta = 1,2 \qquad (12)$$

The third equilibrium equation is

$$(w_{,x}\sigma_{xx} + w_{,y}\sigma_{yx} + \sigma_{zx})_{,x} + (w_{,x}\sigma_{xy} + w_{,y}\sigma_{yy} + \sigma_{zy})_{,y}$$
$$+ (w_{,x}\sigma_{xz} + w_{,y}\sigma_{yz} + \sigma_{zz})_{,z} = 0 \qquad (13)$$

Where w is the lateral displacement. Integrating the above equations in the same fashion as when developing the classical Kirchhoff plate equations

$$N_{\alpha\beta,\beta} = 0 \qquad (14)$$

$$M_{xx,xx} + 2M_{xy,xy} + M_{yy,yy} + N_{xx}\, w_{,xx} + 2N_{xy}\, w_{,xy}$$
$$+ N_{yy}\, w_{,yy} + P = 0 \qquad (15)$$

The nonlinear strains are

$$\begin{aligned} \varepsilon_{xx} &= u^o_{,x} + \frac{1}{2} w^2_{,x} + Zk_{xx} \\ \varepsilon_{yy} &= v^o_{,y} + \frac{1}{2} w^2_{,y} + Zk_{yy} \\ \varepsilon_{xy} &= u^o_{,y} + v^o_{,x} + w_{,x}w_{,y} + Zk_{xy} \end{aligned} \qquad (16)$$

Where k_j are the plate curvatures given by

$$k_{xx} = -w_{,xx} \qquad k_{yy} = -w_{,yy} \qquad k_{xy} = -2w_{,xy} \qquad (17)$$

The constitutive relations in terms of the generalized strains and stress resultants are the well known relations

$$\begin{Bmatrix} N \\ M \end{Bmatrix} = \begin{bmatrix} A & B \\ B & D \end{bmatrix} \begin{Bmatrix} \varepsilon^o \\ K \end{Bmatrix} \qquad (18)$$

Considering a symmetric laminate, for simplicity, and introducing Equation (18) into Equation (15) and B = 0

$$D_{11}\, w_{,xxxx} + 4D_{16}\, w_{,xxxy} + 2(D_{12} + 2D_{66})\, w_{,xxyy} + 4D_{26} w_{,xyyy}$$
$$+ 4D_{26}\, w_{,xyyy} + D_{22}\, w_{,yyyy} = N_x w_{,xx} + 2N_{xy}\, w_{,xy} +$$
$$N_y\, W_{,yy} + p \qquad (19)$$

Next, we will use force function ψ such that the in-plane equilibrium equations are satisfied

$$N_x = \psi_{,yy} \qquad N_y = \psi_{,xx} \qquad N_{xy} = -\psi_{,xy} \qquad (20)$$

Writing the compatibility equation in terms of the mid-surface strains

$$\varepsilon^o_{x,yy} + \varepsilon^o_{y,xx} - \varepsilon^o_{xy,xy} = w^2_{,xy} - w_{,xx}\, w_{,yy} \qquad (21)$$

Introducing (20) into (18) and substituting the reference surface strains ε^o_{ij} into (21)

$$A^{-1}_{22}\, \psi_{,xxxx} - 2A^{-1}_{26}\, \psi_{,xxxy} + \left(2A^{-1}_{12} + A^{-1}_{66}\right) \psi_{,xxyy} - 2A^{-1}_{16}\, \psi_{,xyyy} +$$
$$A^{-1}_{11}\, \psi_{,yyyy} = w^2_{,xy} - w_{,xx} w_{,yy} \qquad (22)$$

Equations (19) and (22) define a set of coupled partial differential equations. These are the postbuckling nonlinear equations of thin laminated plates.

REFERENCES

1. Adams D.F.," Inelastic Analysis of a Unidirectional Composite Subject to Transverse Normal Loadin ", J. Composite Mats., Vol.4, pp.310, 1970.

2. Zvi Hashin, Debal Bagchi and B. Walter Rosen," Nonlinear Behavior of Fiber Composite Laminates", NACA CR- 2313, 1974.

3. Smith G.F. and R.S. Rivlin," The Strain Energy Function for Anisotropic Elastic Materials", Trans. AMS.,Vol.88, pp. 175-193, 1958.

4. Hong T. Hahn and Stephen W. Tsai," Nonlinear Elastic Behavior of Unidirectional Composite Laminates", J. Composite Mats., Vol.7,pp.102, 1973.

5. C.Y. Chia and M.K. Prabhakara," Nonlinear Analysis of Orthotropic Plates", J. Mech. Eng. Sci., Inst. Mech. Eng.(London), pp. 133-138,1975.

6. M.K. Prabhakara and C.Y. Chia," Postbuckling of Angle-Ply and Anisotropic Plates", Ing. Arch., Vol.45,springer-Verlag KG (Berlin),pp. 131-140, 1976.

7. M. Stein," Effect of Transverse Shearing Flexibility on Postbuckling of Plates in Shear", AIAA J.,Vol.27, No.5,pp652-655,1989.

8. A.K. Noor and J.M. Peters," Multiple-Parameter Reduced Basis Technique for Bifurcation and Postbuckling analysis of Composite Plates", Int. J. Num. Meth. Eng., Vol.19,No.12,pp. 1783-1803,1983.

9. J.H. Stranes Jr. and M. Rouse," Postbuckling and Failure Characteristics of Selected Flat Rectangular Graphite-Epoxy Plates Loaded in Compression", Proceeding of the 22-nd AIAA/ASME/ASCE/AHS Structures, Structural Dynamics and Material Conference, Atlanta,GA,AIAA Cp. 811, pp. 423-434,1981.

10. H. Wely, The Classical Groups, Princeton University press, p. 36,53,276 , 1946.

11. Crisfield M.A.," A Fast Incremental/Iterative Solution Procedure that Handels ' Snap-Through' ", Computers and Structures, 13, pp 55-62, 1978.

12. ABAQUS Computer Code, Version 4.7, Hibitt, Karlsson and Sorensen Inc., Providence, R.I.,1988.

13. S.S. Wang and A. Dasgupta," Development of Iosipescu-Type for determining in-Plane Shear Properties of Fiber Composite Materials: Critical Analysis and Experiment", Polymer Group, University of Illinois at Urbana-Champaign, UILU-ENG-86-5021, 1986.

14. A. Miyase, Experimental Study at the National Center for Composite Materials Research, to be published.

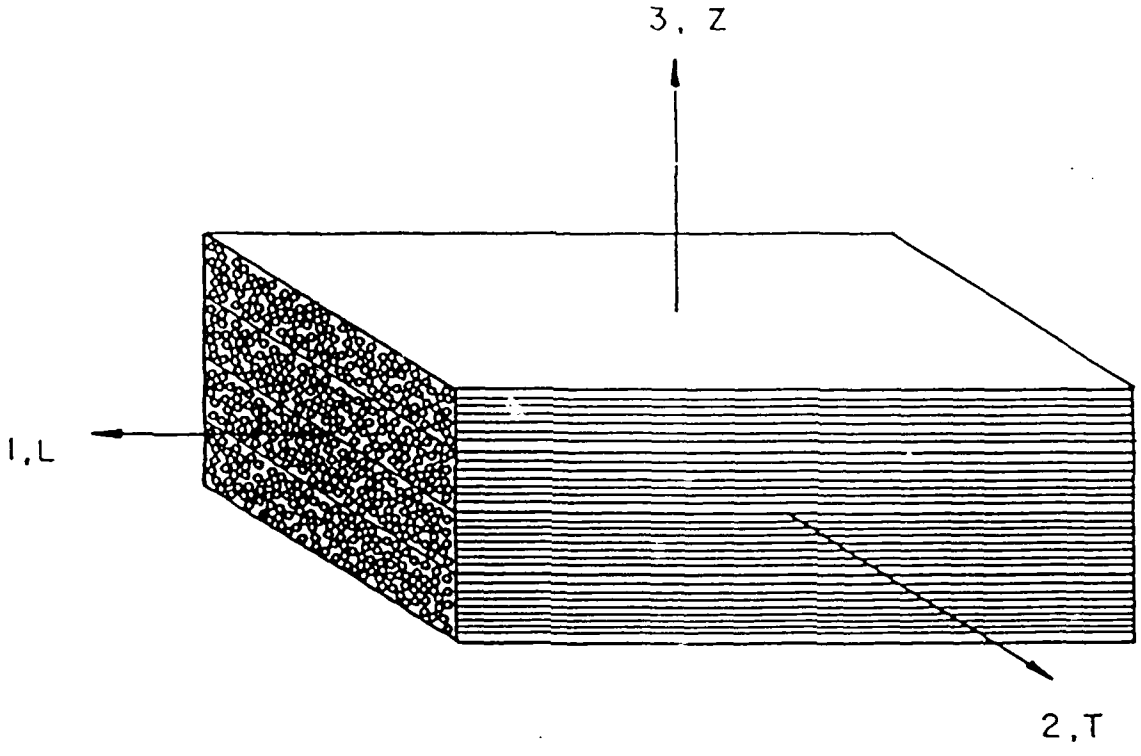

Fig.1 - Unidirectional fiber composite material.

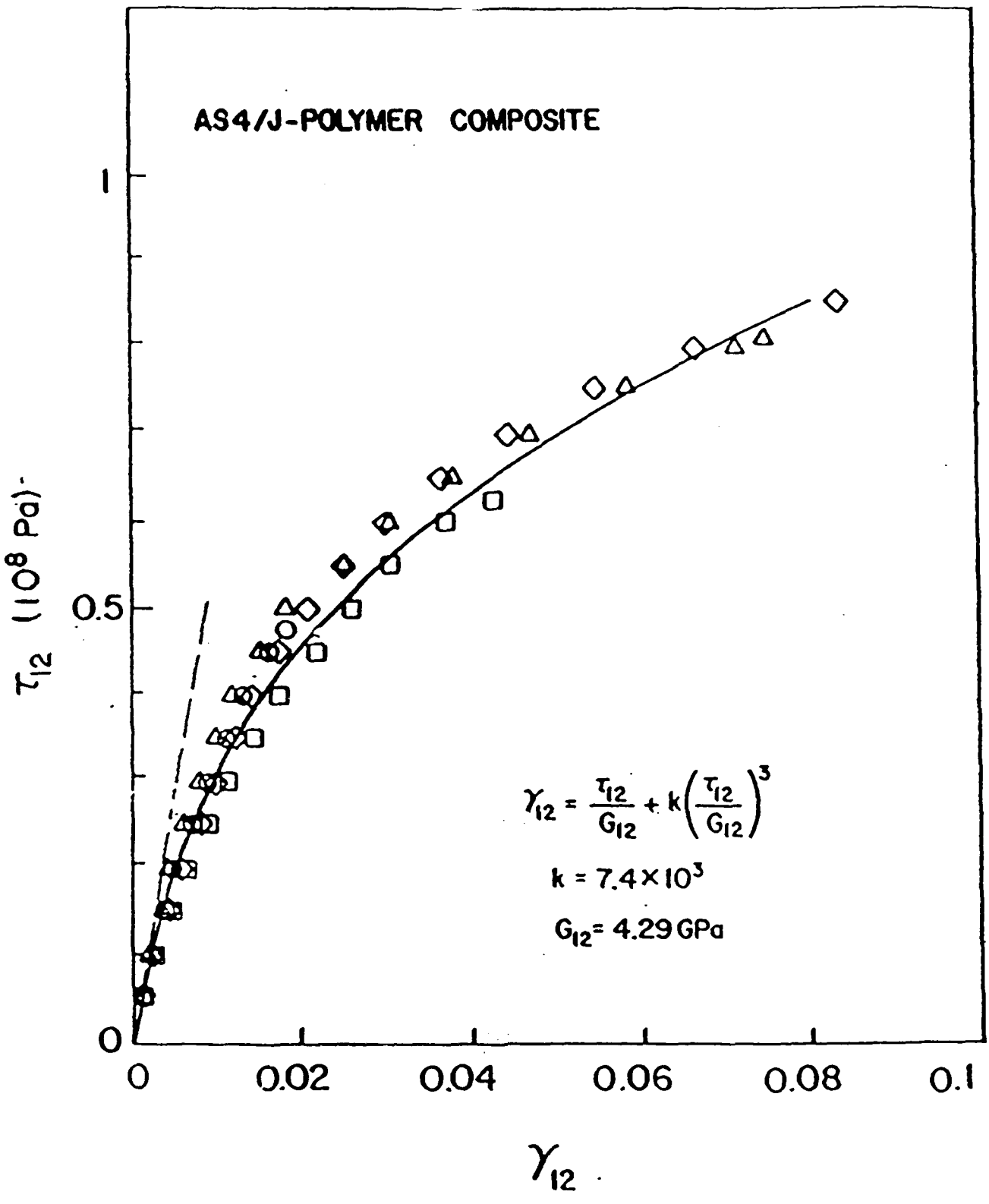

Fig.2.-.Axial shear stress-strain curve, ref. [13].

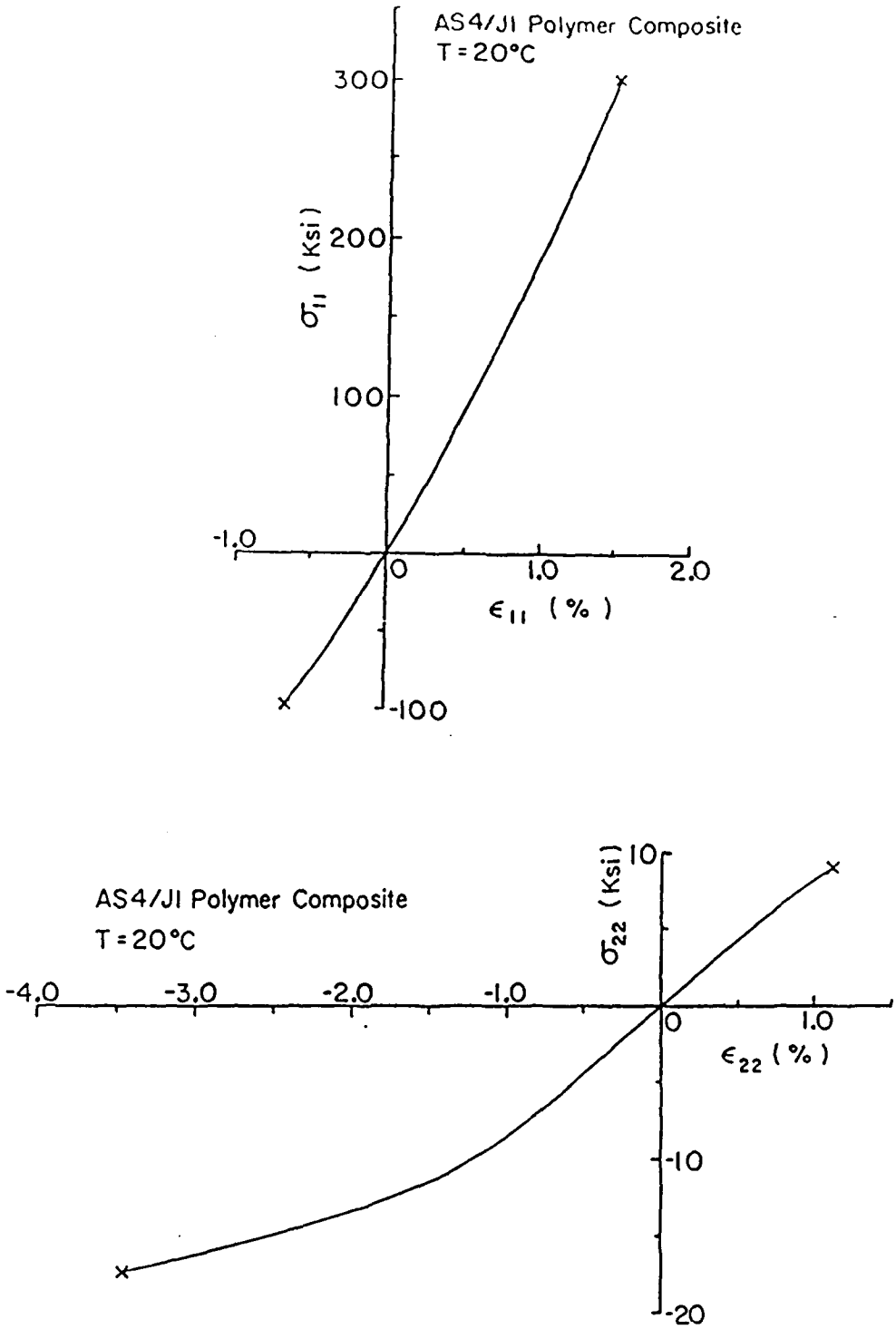

Fig.3.-.Transverse and axial stress-strain curves, ref. [14].

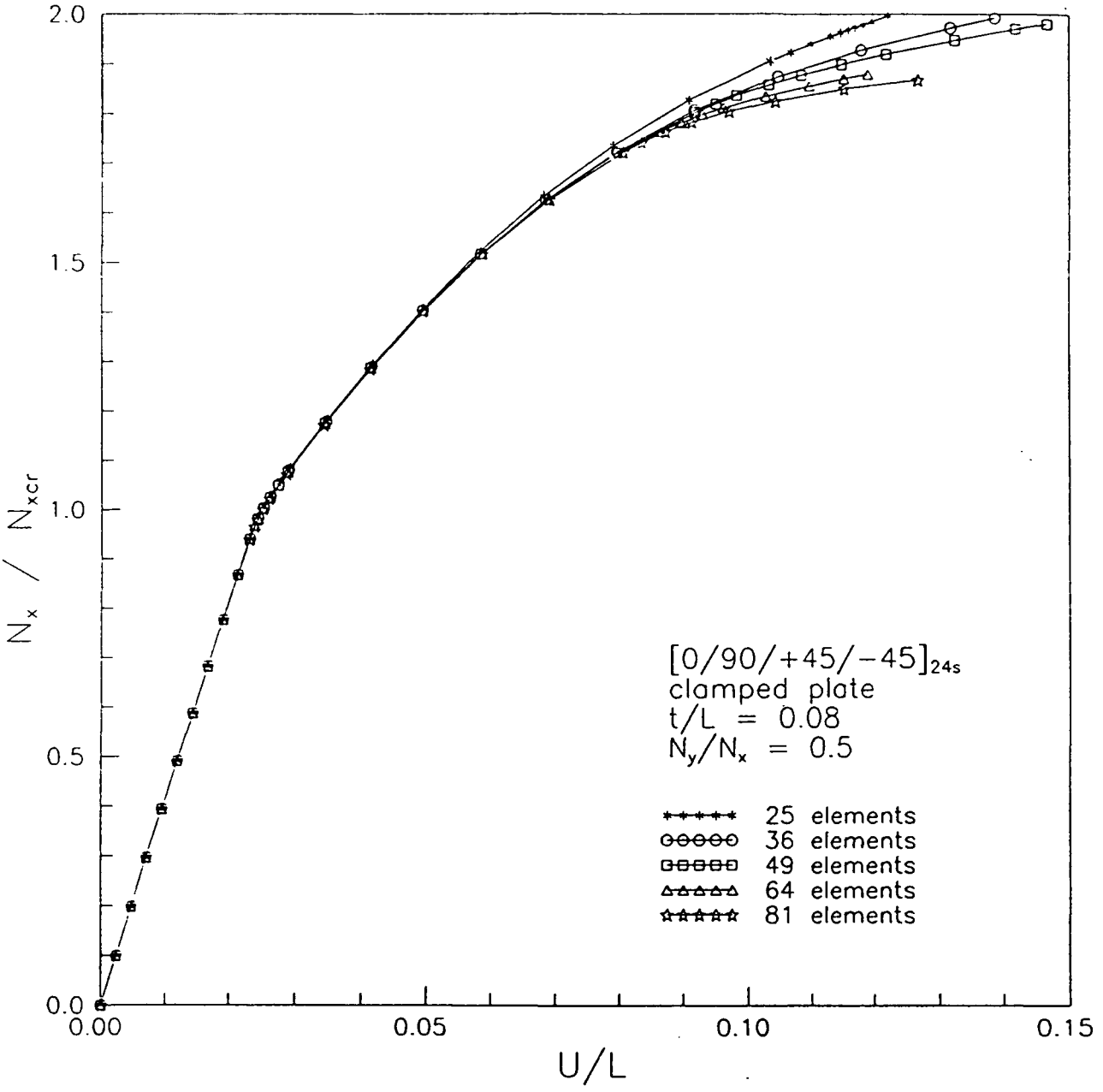

Fig.4 - Convergence study of postbuckling response of clamped plate in the form of plate end-shortening.

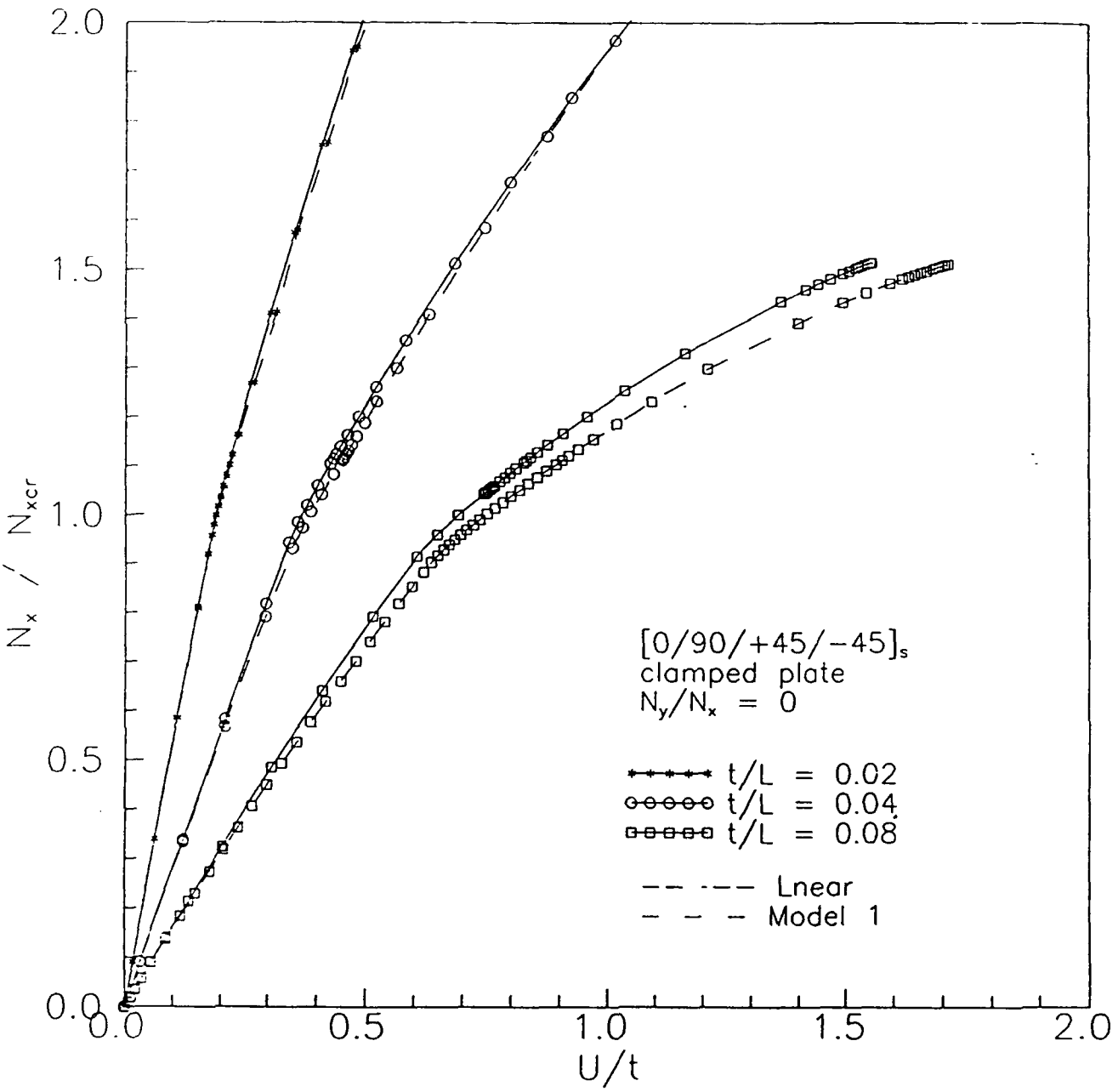

Fig.5 - **Effect of laminate thickness on plate postbuckling behavior for linear and nonlinear fiber composite materials. End-shortening versus axial load (clamped plate, 1.% imperfection, N_y=0).**

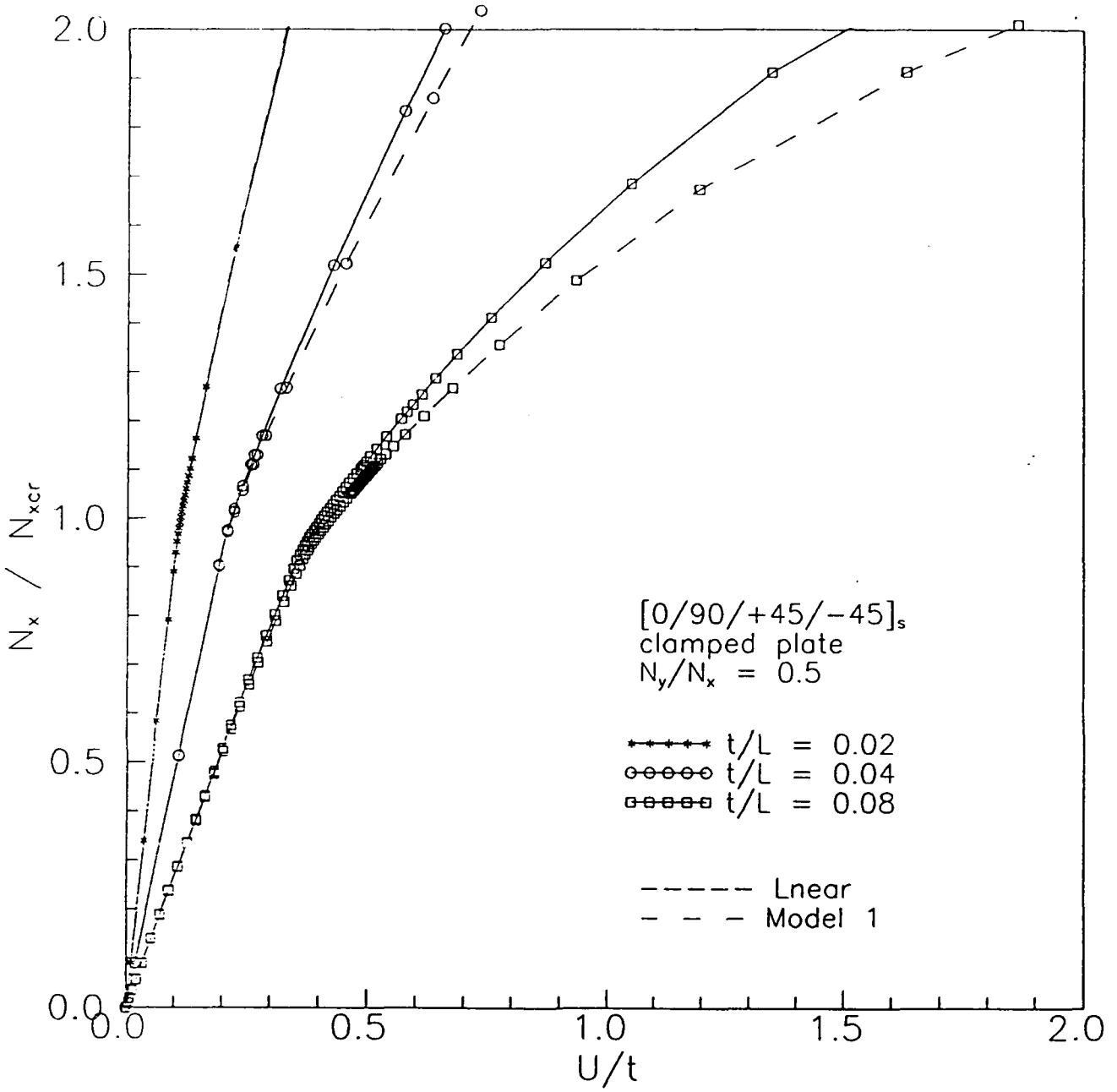

Fig.6 - **End-shortening of laminates with different aspect-ratios for linear and nonlinear materials.(Clamped plate, 1.% imperfection,** N_Y/N_X=0.5).

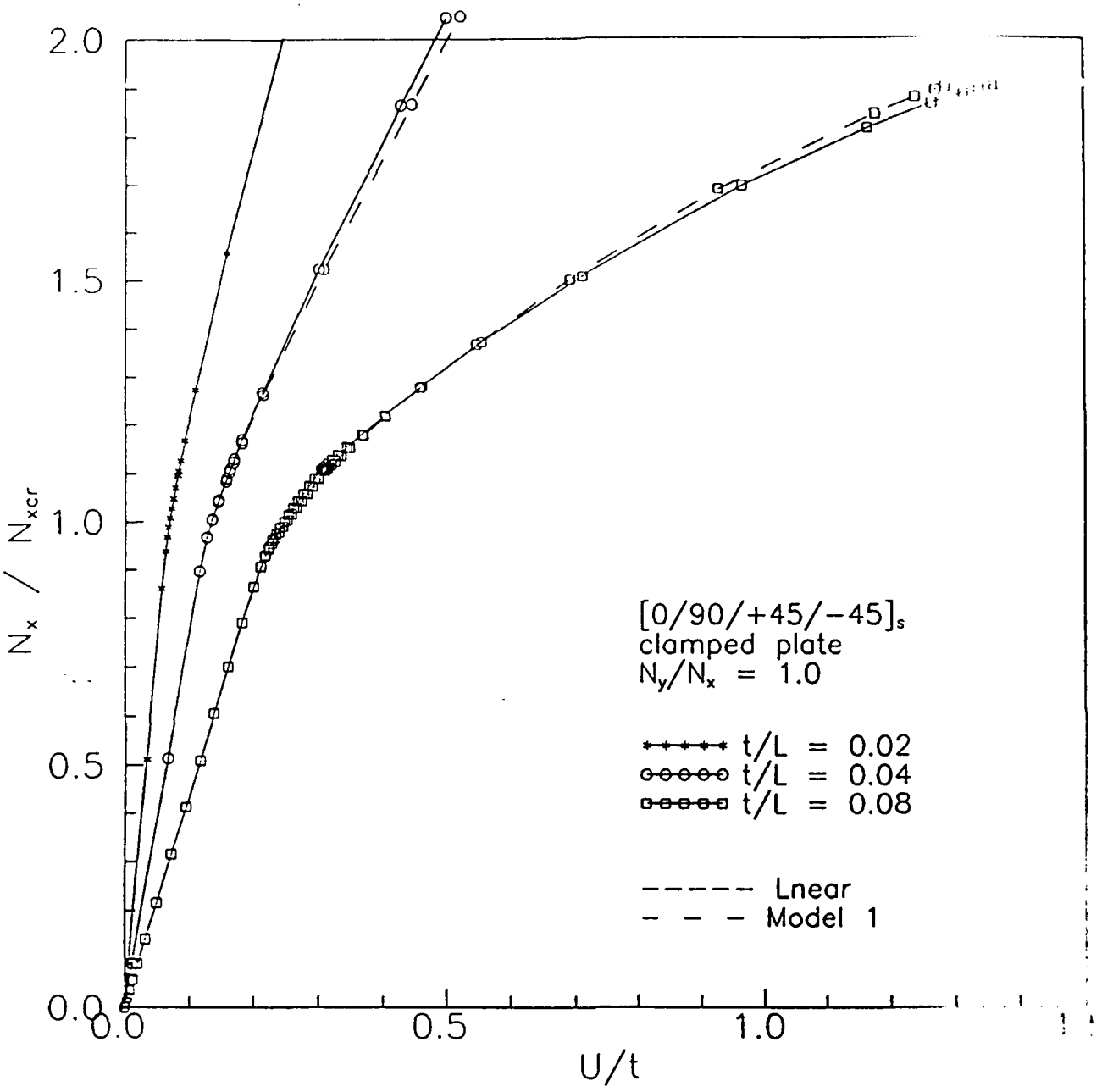

Fig.7 - Effect of laminate thickness on plate postbuckling behavior for linear and nonlinear fiber composite materials. End-shortening versus axial load. (Clamped plate, 1.% imperfection, N_y/N_x=1.).

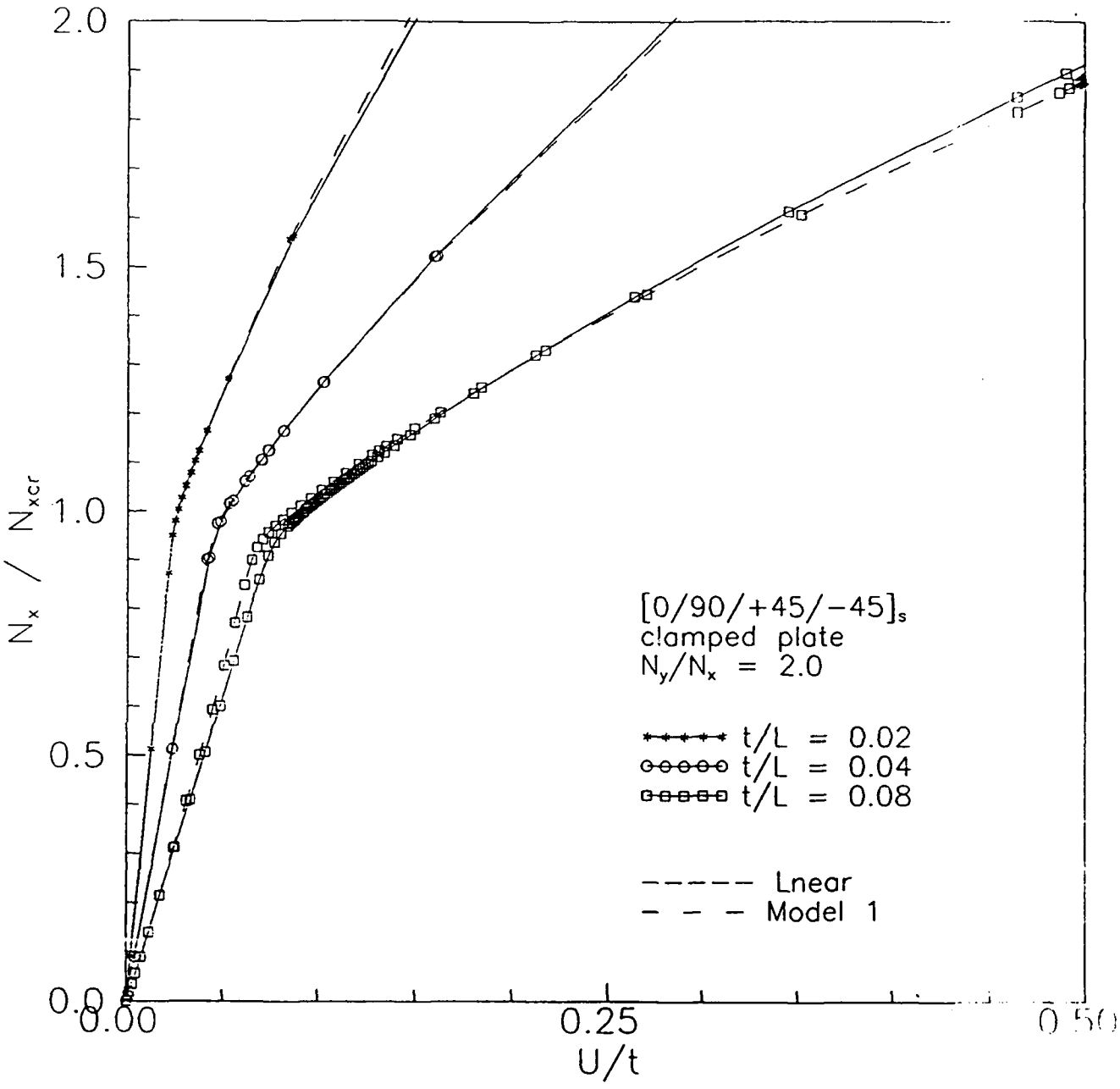

Fig.8 - Effect of laminate thickness on plate postbuckling behavior for linear and nonlinear fiber composite materials. End-shortening versus axial load. (Clamped plate, 1.% imperfection, N_y/N_x=2).

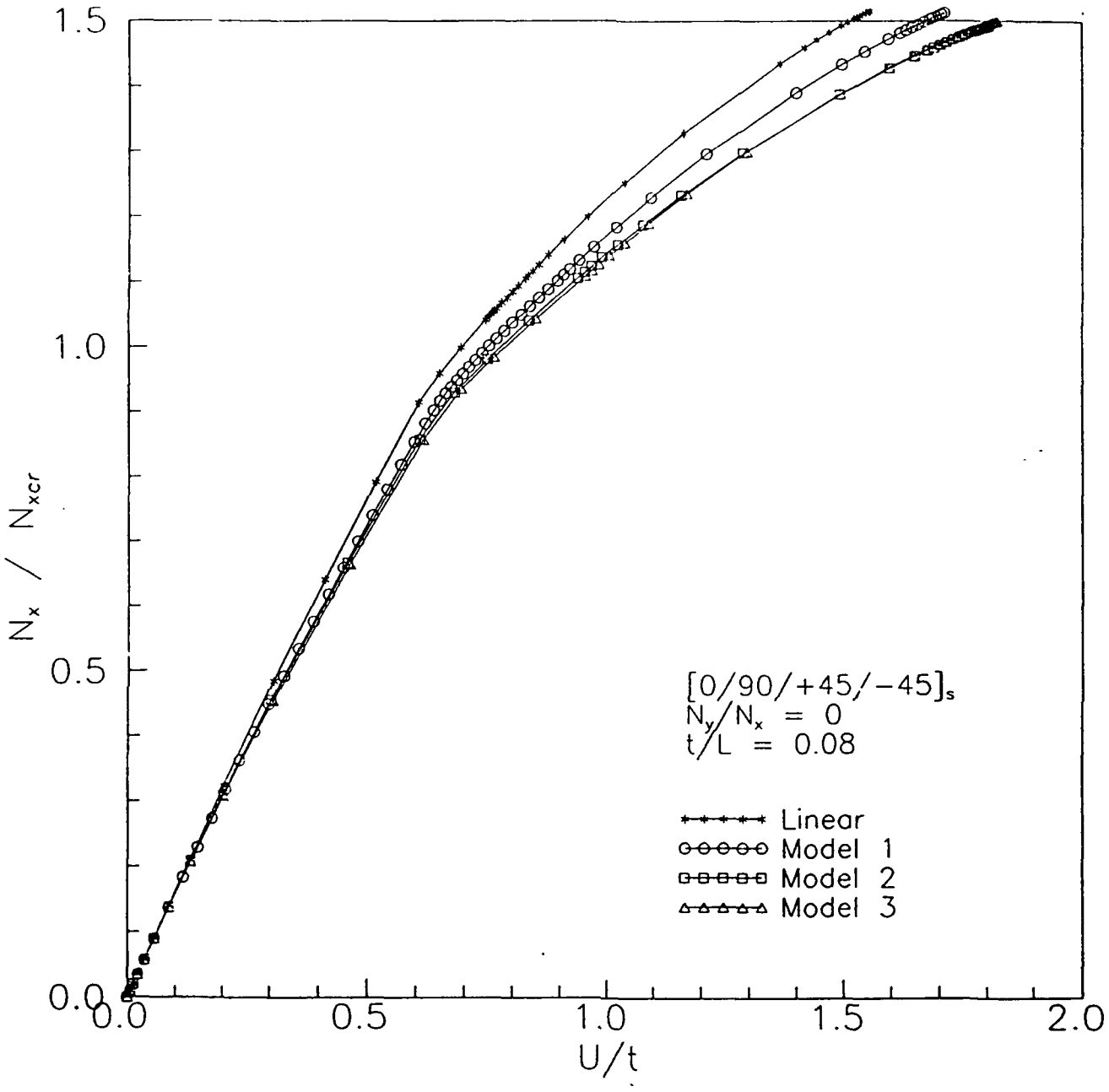

Fig.9 - End-shortening of thick-section laminated plate for linear and nonlinear material models. (1.% imperfection, N_y=0, t/L=0.08).

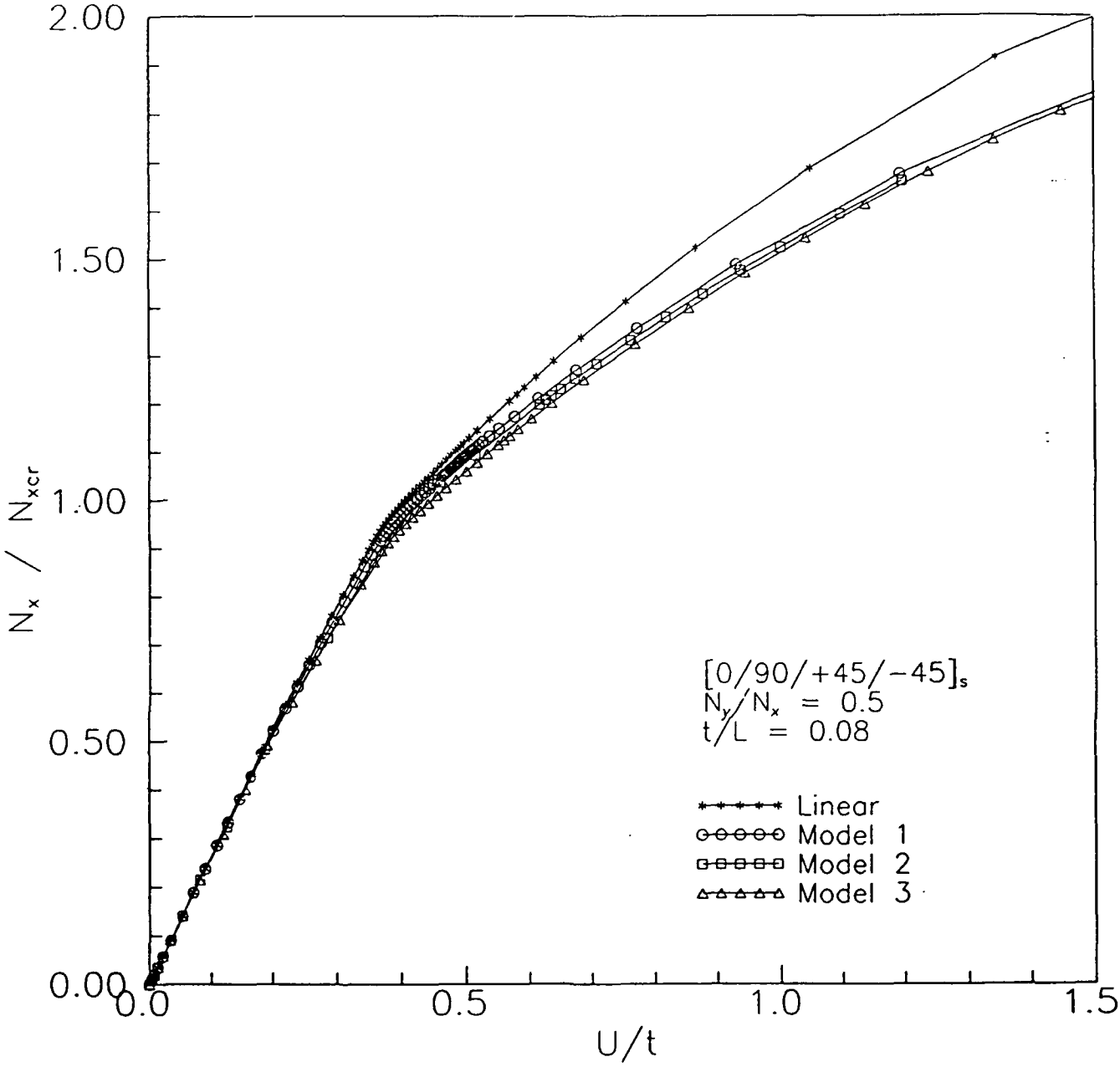

Fig.10 - End-shortening of thick section laminated plate for linear and nonlinear material models. (1.% imperfection, N_y/N_x=0.5,t/L=0.08).

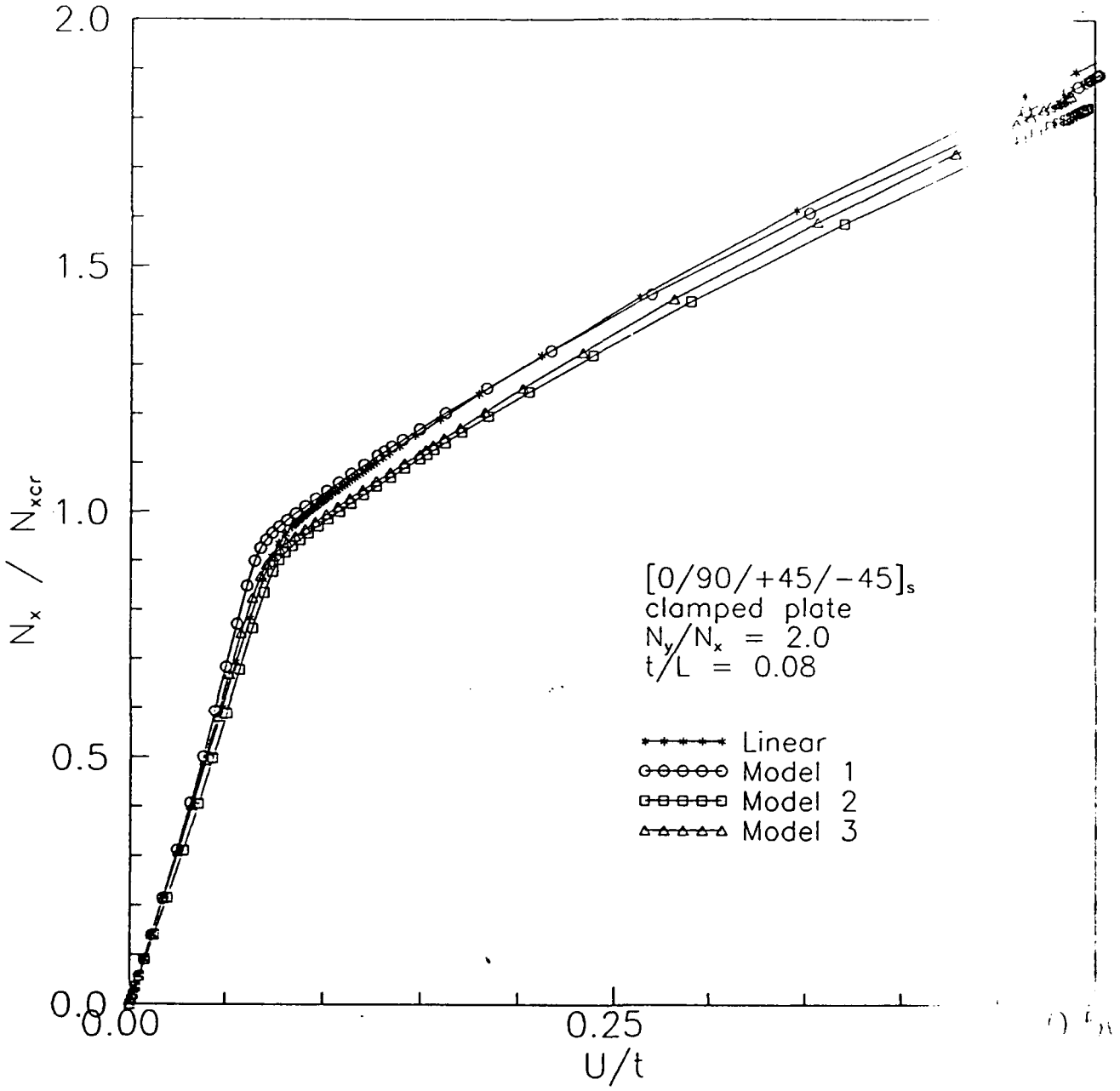

Fig.11 - End-shortening of thick-section laminated plate for linear and nonlinear material models. (1.% imperfection, N_y/N_x=2., t/L=0.08)

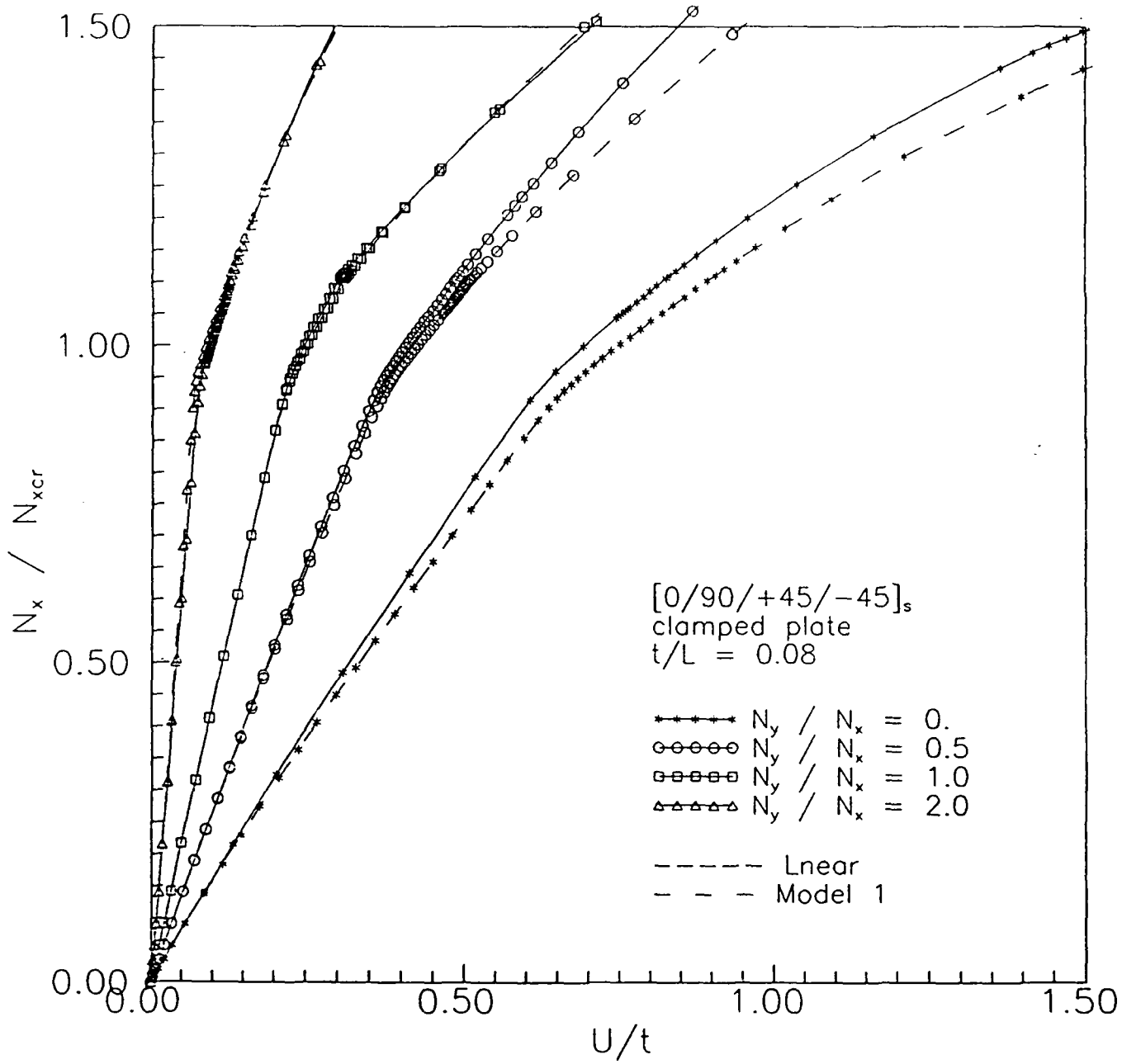

Fig.12 - Effect of stress-biaxiality ratio on postbuckling response for linear and nonlinear material models. (1.% imperfection, t/L=0.08).

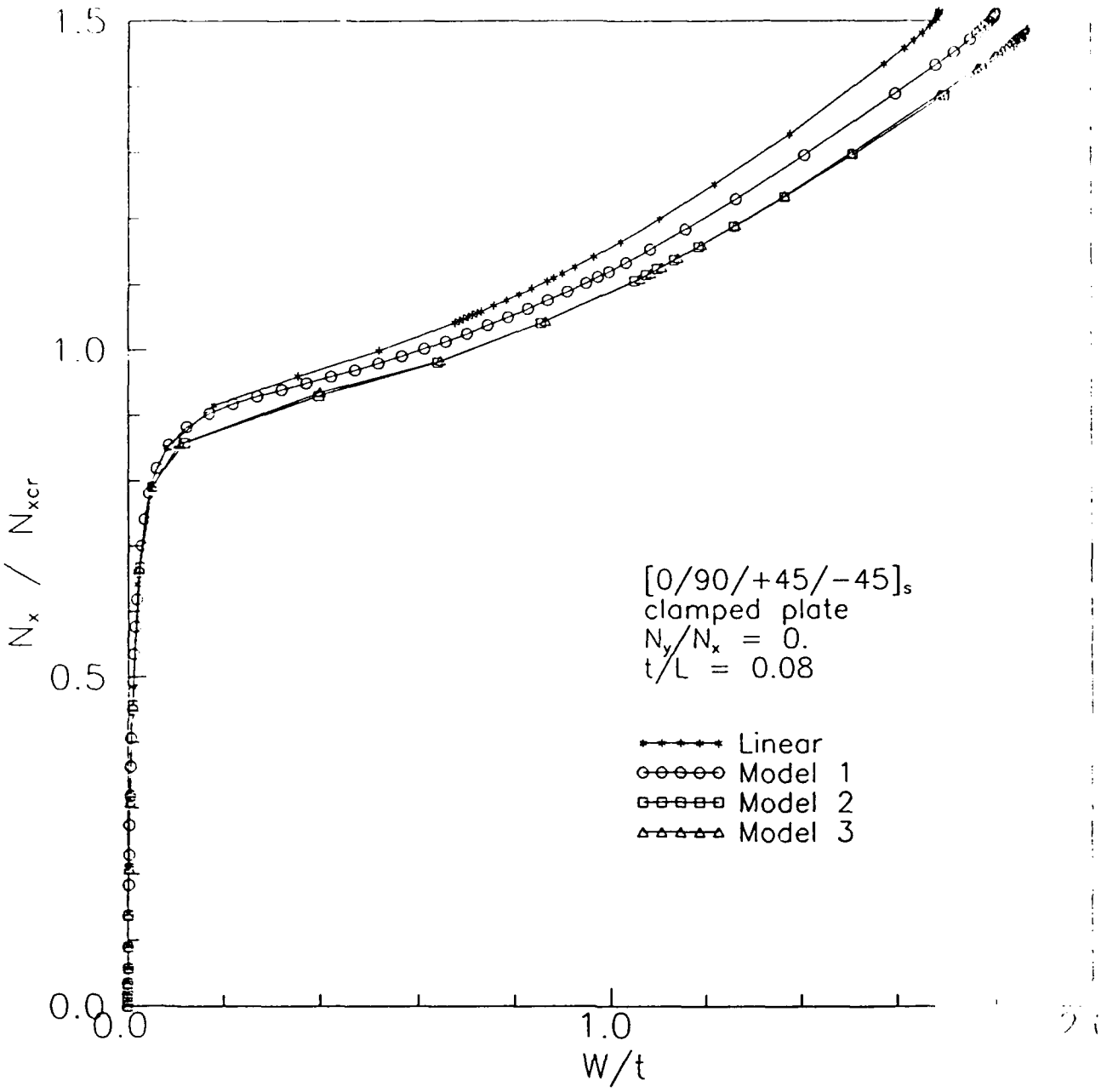

Fig.13 - **Postbuckling load and plate central deflection for thick section and different material models. (1.% imperfection, N_y/N_x=0, t/L = 0.08).**

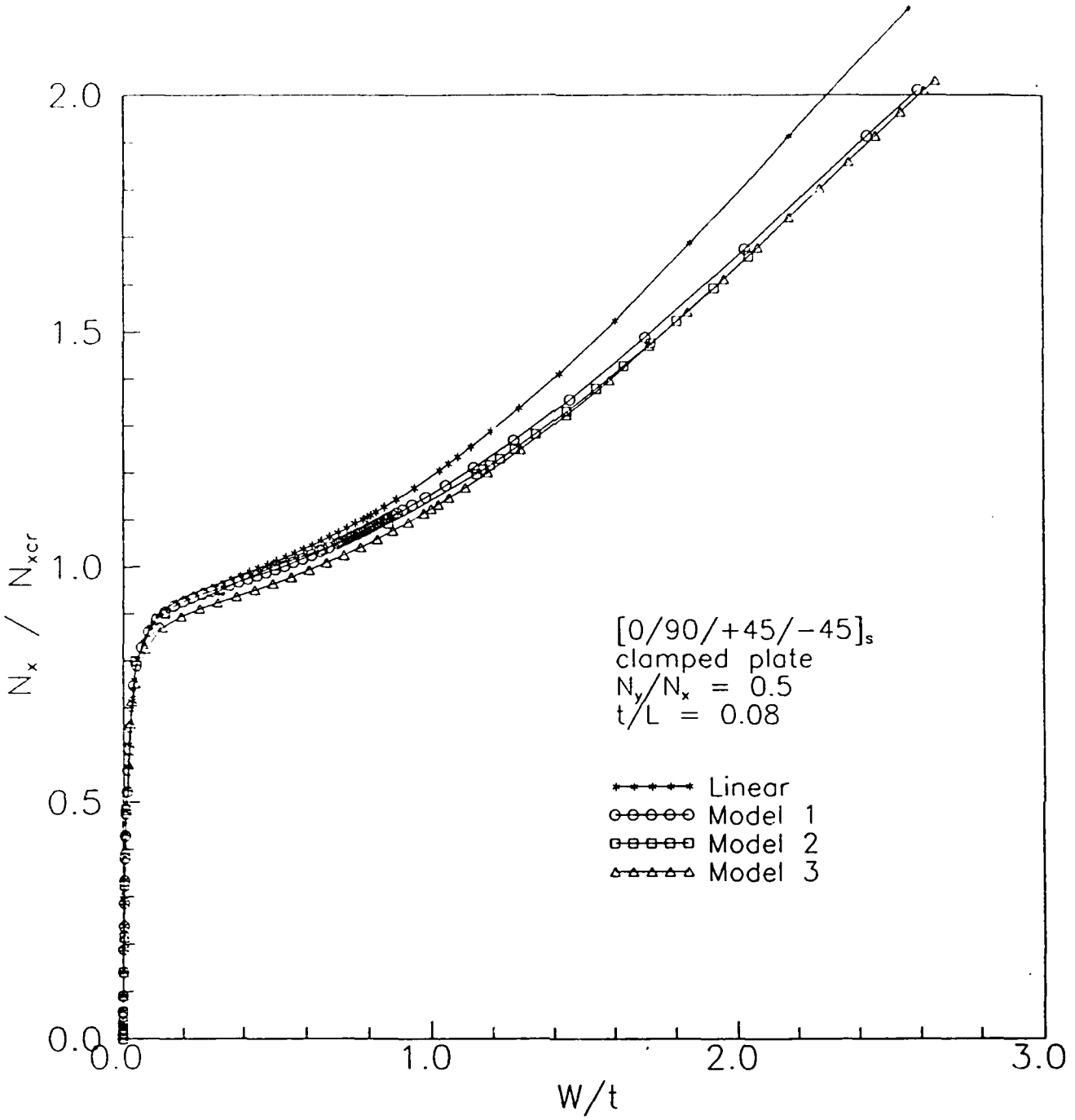

Fig.14 - Postbuckling load and plate central deflection for thick-section and different material models. (1.% imperfection, N_y/N_x=0.5, t/L=0.08).

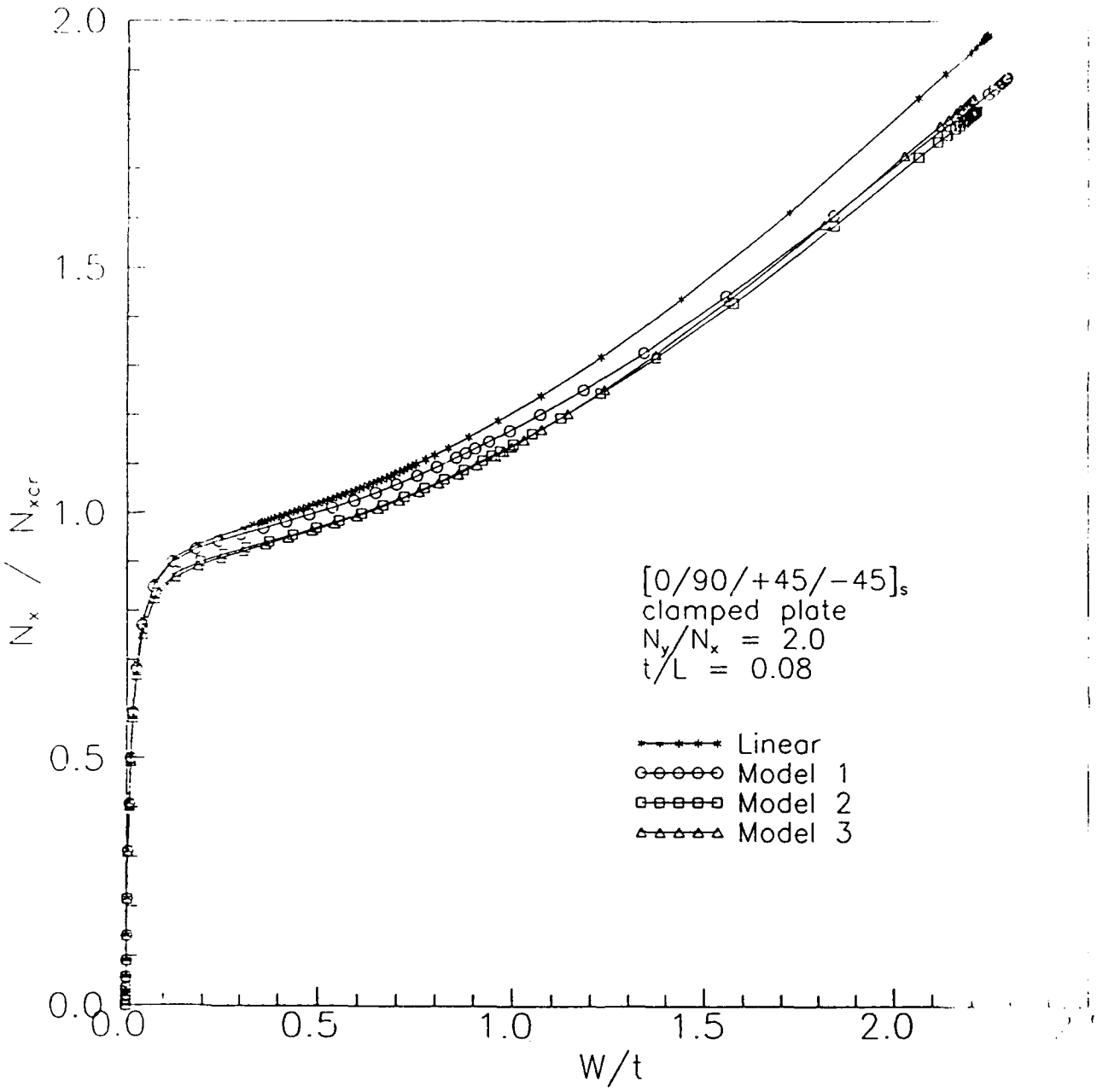

Fig.15 - **Postbuckling load and plate central deflection for thick section and different material models.(1.% imperfection, N_y/N_x=2., t/L=0.08)**

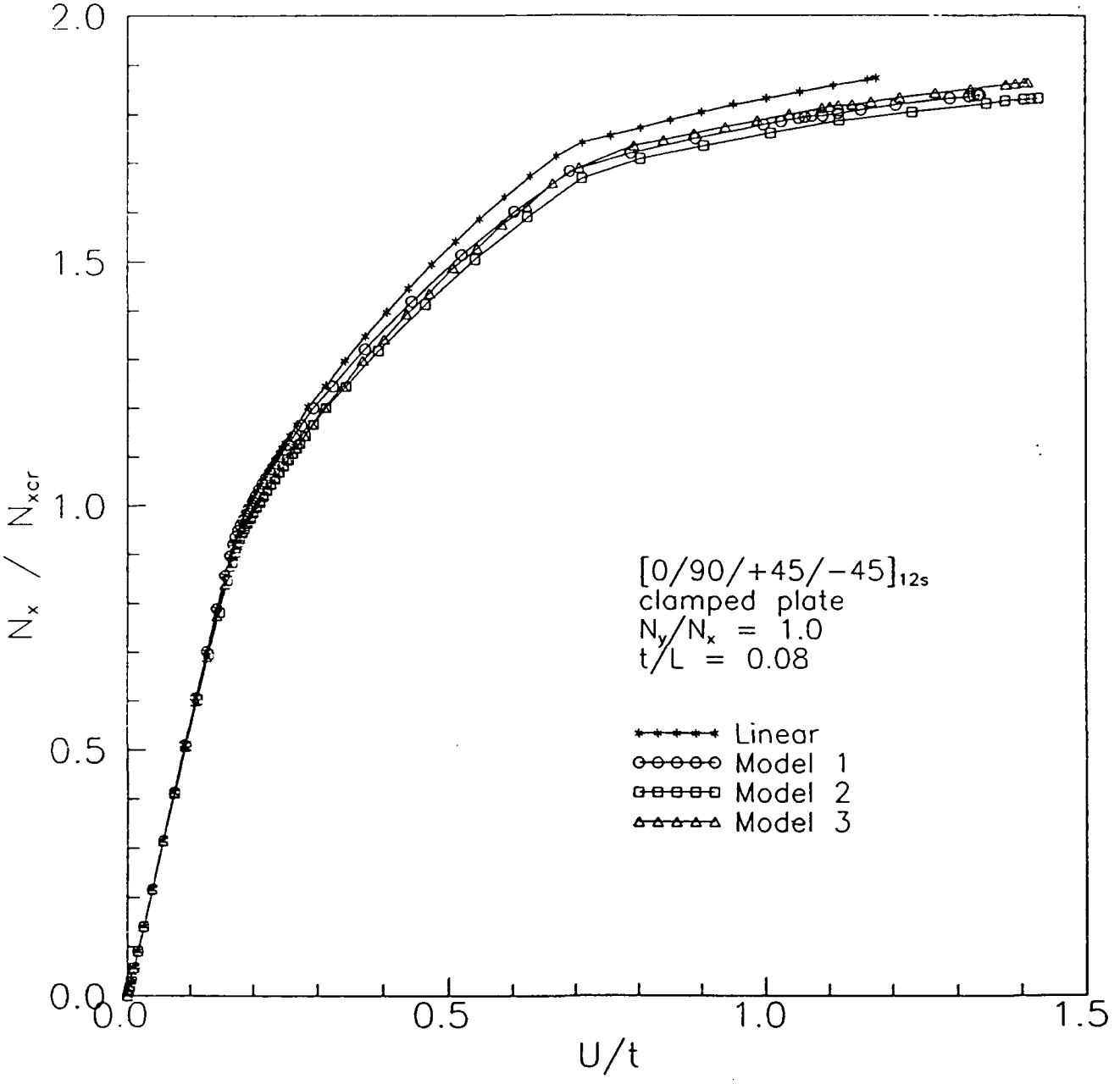

Fig.16 - **End-shortening of thick-section multi-layered plate for linear and nonlinear material model (Clamped plate, 1.% imperfection, N_y/N_x-1.).**

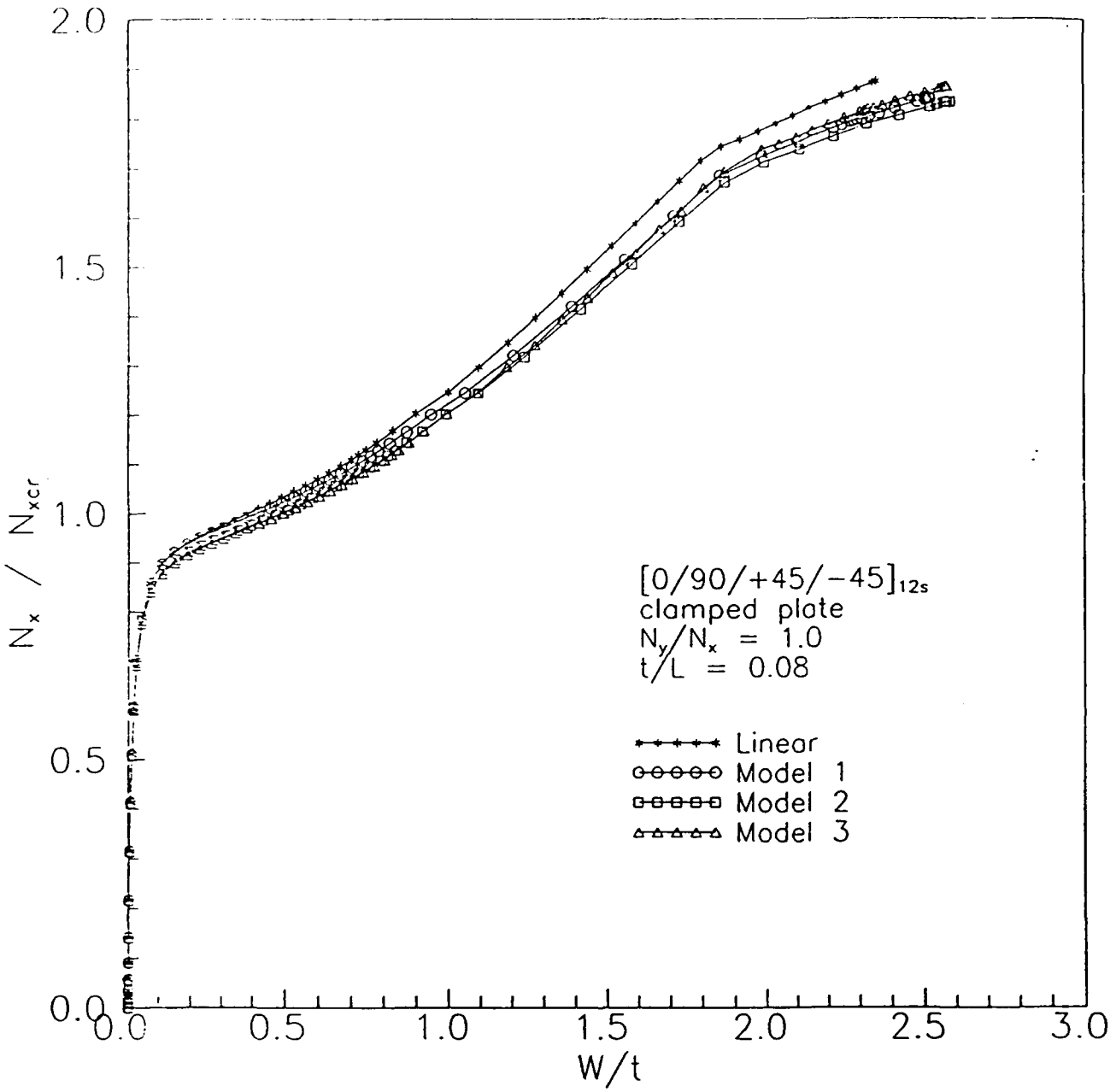

Fig.17 - **Lateral deflection of multi-layered thick plate for different material models. (Clamped plate, 1.% imperfection, N_y/N_x=1., t/L=0.08).**

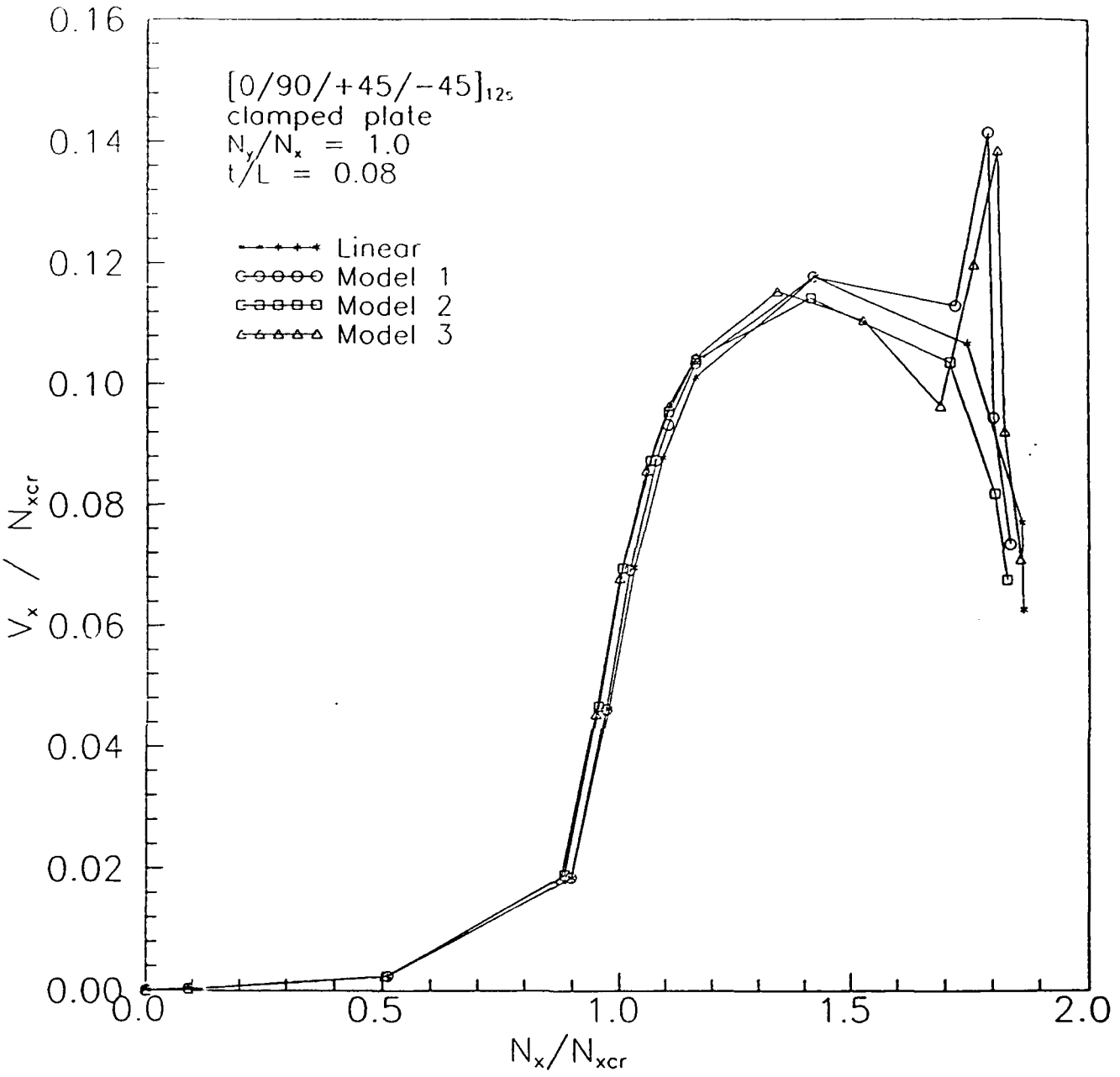

Fig.18 - Transverse shear behavior in a clamped [0/90/±45]izs plate under biaxial compression.

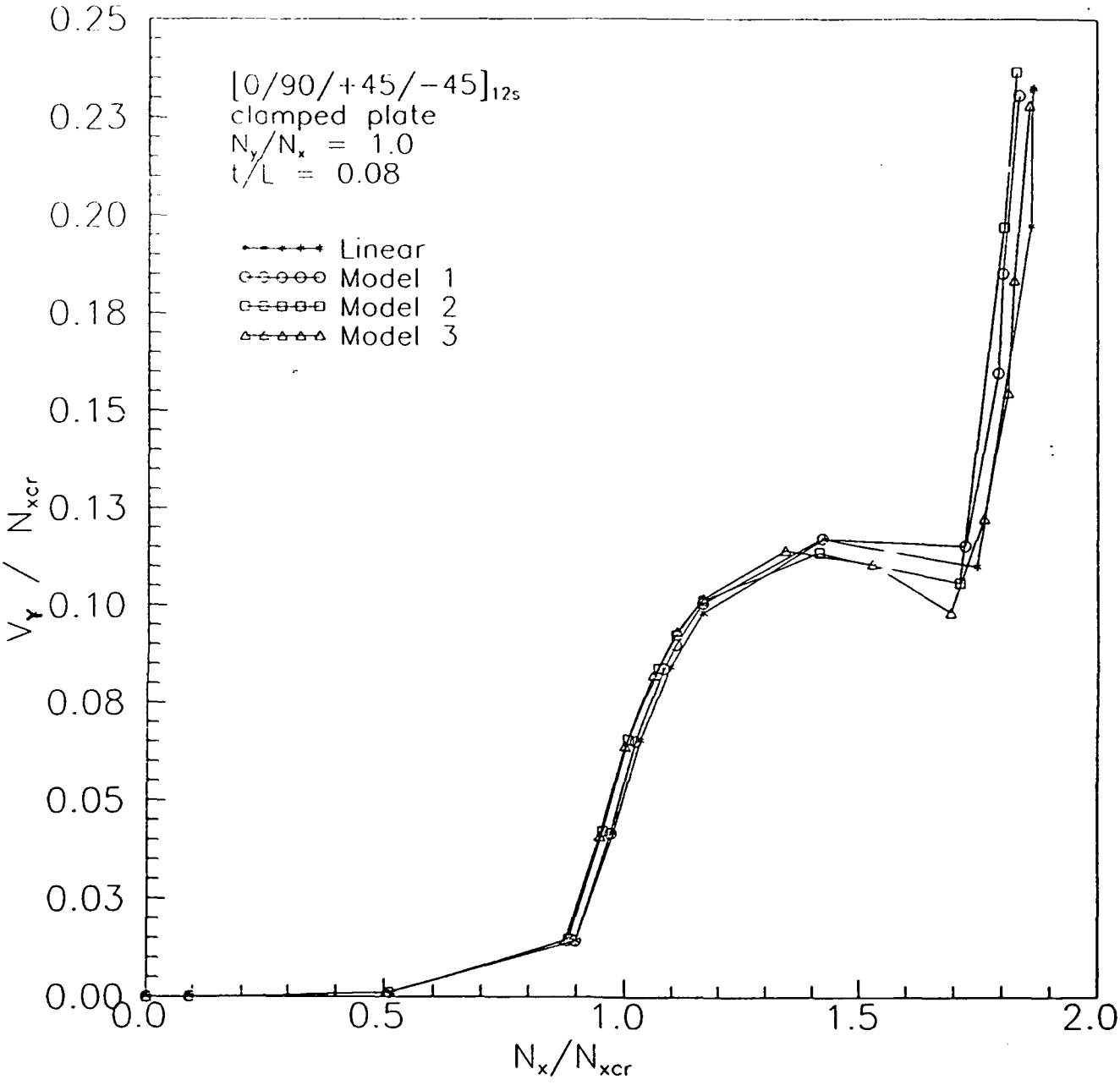

Fig.19 - Transverse shear behavior in a clamped $[0/90/\pm45]_{12s}$ plate under biaxial compression.

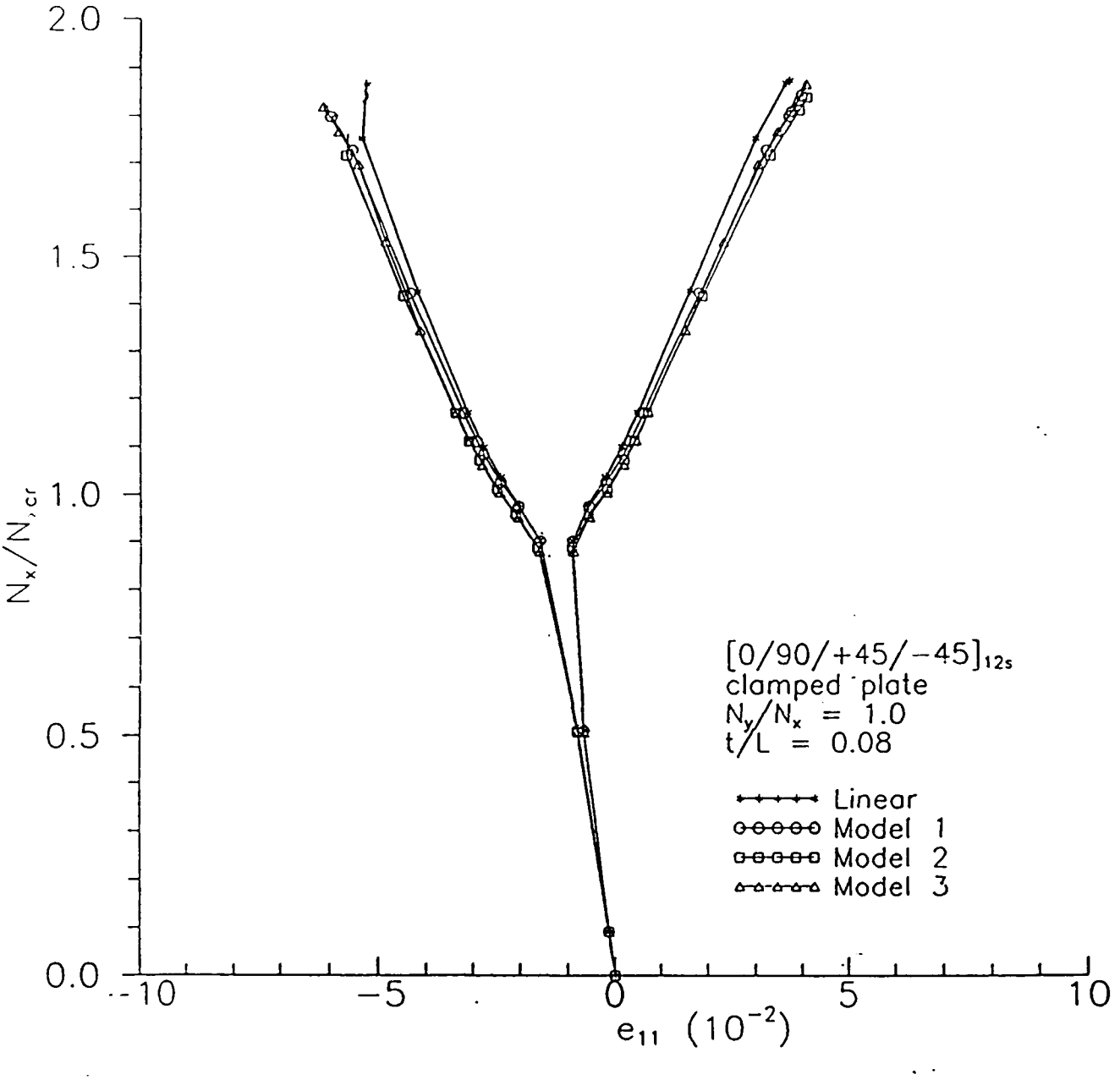

Fig.20 - **Axial strain behavior of the top and bottom layers at the plate center.**